Original Contribution

Kurume Medical Journal, 57, 91-100, 2010

Utility of Multidetector Row CT in Diagnosing Branch Duct IPMNs of the Pancreas Compared with MR Cholangiopancreatography and Endoscopic Ultrasonography

SHUNJI ARIKAWA, MASAFUMI UCHIDA, JUN UOZUMI, JUN SAKODA, HAYATO KAIDA, YUKIKO KUNOU, YASUMITSU HIROSE, TOSHI ABE, NAOFUMI HAYABUCHI, YOSHIKI NAITO*, YOSHINOBU OKABE**, HIDEYA SUGA** AND HISAFUMI KINOSHITA†

Departments of Radiology, Pathology, Medicine** and Surgery†, Kurume University School of Medicine, Kurume 830-0011, Japan*

Received 25 May 2010, accepted 1 September 2010

Edited by MINORU YAGI

Summary: This study aimed to compare the usefulness of multidetector row CT (MDCT), MR cholangiopancreatography (MRCP), and endoscopic ultrasonography (EUS) in diagnosing branch duct intraductal papillary mucinous neoplasms (IPMNs) of the pancreas. Imaging and pathological findings were retrospectively evaluated for 25 patients with branch duct IPMNs of the pancreas who underwent surgical resection (13 adenomas, 4 borderline lesions, and 8 carcinomas). MDCT and MRCP were performed on all 25 patients, whereas EUS was performed on 22 patients. MDCT and MRCP were used to identify features predictive of malignancy, including carcinoma, borderline lesions, and the presence of thickened irregular walls/septa or a solid mass. EUS was used to identify the presence of intramural nodules or a solid mass. Correlations between histopathology and maximum diameter of the main pancreatic duct (MPD) or cyst size detected by MDCT and MRCP were also examined. Presence of a solid mass was highly correlated with malignancy with all imaging methods (MDCT; P=0.001, MRCP; P=0.008, EUS; P<0.001, respectively). Presence of thickened irregular walls/septa on MDCT correlated well with malignancy (P=0.019). In contrast, presence of thickened irregular walls/septa on MRCP and intramural nodules on EUS did not correlate with malignancy. No significant correlation was found between malignancy and average maximum MPD diameter or cyst size (P>0.05), though values tended to be larger in malignant tumors. Our results suggest that the presence of thickened irregular walls/septa or a solid mass on MDCT are highly correlated with malignancy, and that MDCT is useful for diagnosis of branch duct IPMNs of the pancreas.

Key words intraductal papillary mucinous neoplasms (IPMNs) of the pancreas, multidetector row computed tomography (MDCT), magnetic resonance cholangiopancreatography (MRCP), endoscopic ultrasonography (EUS)

INTRODUCTION

Intraductal papillary mucinous neoplasms (IPMNs) of the pancreas are characterized by massive production and retention of mucin in the pancreatic duct and interstitium, dilation of the papilla of Vater caused by

Correspondence: Shunji Arikawa, Department of Radiology, Kurume University School of Medicine, 67 Asahi-machi, Kurume 830-0011, Japan. Tel: +81-942-31-7576 Fax: +81-942-32-9405 E-mail: aririn@med.kurume-u.ac.jp

Abbreviations: CPR, curved planar reformatting; ERCP, endoscopic retrograde cholangiopancreatography; EUS, endoscopic ultrasonography; HU, hounsfield units; IPMNs, intraductal papillary mucinous neoplasms; kVp, kilovolts; mAs, milliampere seconds; MDCT, multidetector row CT; MIP, maximum intensity projection; MPD, main pancreatic duct; MPR, multiplanar reformatting; MRCP, magnetic resonance cholangiopancreatography; RARE, rapid acquisition with relaxation enhancement; 3D-TSE, three-dimensional turbo spin echo; WHO, World Health Organization.

mucinous flow, little tendency for infiltration, and good prognosis [1]. Pathologically, IPMNs can manifest with different degrees of cellular atypia, ranging from hyperplasia, to adenoma with varying degrees of dysplasia or invasive carcinoma. IPMNs can be classified as either main duct IPMNs or branch duct IPMNs based on imaging studies [2,3]. Main pancreatic duct types are indicated for surgery regardless of the presence of intramural nodules; cyst diameter, main pancreatic duct diameter, and the presence of intramural nodules are considered important findings for branch duct types. However, the intramural nodule size diagnostic of malignancy and diagnostic testing methods for branch duct types vary among reports, and currently are not uniform.

Many imaging techniques can be used to evaluate branch duct IPMNs of the pancreas, including CT, magnetic resonance cholangiopancreatography (MRCP), endoscopic retrograde cholangiopancreatography (ERCP), and endoscopic ultrasonography (EUS). MRCP is currently being investigated as the preferred imaging modality for diagnosis and follow-up of branch duct IPMNs of the pancreas [4,5]. CT remains the most commonly used imaging method, as well as the initial method of choice for evaluating patients with pancreatic disease. Multidetector row CT (MDCT) involves the use of very thin collimation for the acquisition of high-resolution images during multiple phases of contrast enhancement, resulting in enhanced evaluation of the communication between the main pancreatic duct (MPD) and cystic lesion, and simultaneous evaluation of the pancreatic parenchyma and pancreatic duct [6]. The purpose of this study was to compare the predictive features of malignancy identified by MDCT, MRCP, and EUS in branch duct IPMNs of the pancreas, as well as to examine the correlations between histopathology and maximum MPD diameter or cyst size detected by MDCT and MRCP.

MATERIALS AND METHODS

Patients

Forty-five (45) patients at our institution were diagnosed with branch duct IPMNs of the pancreas based on ERCP findings between August 2003 and December 2008. Of the 45 patients, 25 underwent surgical resection without follow-up, and the diagnosis of IPMNs of the pancreas was confirmed by pathologic specimen in all cases. The remaining 20 patients were selected for follow-up due to age, poor general condition, or refusal to undergo a surgical procedure. Thus, our study population included 25 patients (20 men and 5 women; average age, 65.2 years; age range, 37-84 years). MDCT and MRCP were performed on all 25 patients. EUS was performed on 22 patients; 3 of the 25 patients refused EUS. Informed consent for participation in the study was obtained from each patient or guardian as part of the protocol approved by the institutional clinical subpanel on human studies at our university hospital.

MDCT technique

Contrast-enhanced dynamic CT scans (unenhanced, arterial, pancreatic parenchymal, portal, and delay phases) were performed with a 16-detector row scanner (Light Speed Ultra; GE Healthcare, Milwaukee, WI, USA). All patients fasted for at least 5 hrs prior to examination and received 100 mL of nonionic contrast material (Iopamidol, 370 mgI/mL; Bayer Schering Pharma, Berlin, Germany) intravenously by means of a power injector (Auto Enhance A-50; Nemoto-Kyorin-Dou, Tokyo, Japan) at a rate of 4 mL/s. Scans were acquired in the craniocaudal direction with the following parameters: pitch of 1.375:1, 0.7-sec scanning time per rotation, table speed of 13.75-27.50 mm/rotation, and detector configuration of 0.625-1.25×16 mm. Peak tube voltage was 120 kilovolts (kVp), and the current-time product was 300-440 milliampere seconds (mAs). Using a bolus-triggered technique (SmartPrep; GE Healthcare) in which the cursor was placed on the aorta and the threshold set at 200 Hounsfield units (HU), the arterial, pancreatic parenchymal, portal, and delay phases were initiated at 5, 20, 40, and 70 seconds, respectively, after the trigger threshold was achieved.

CT data for each phase were retrospectively reconstructed with a 0.625 to 1.25 mm section thickness at an interval of 0.625 to 1.25 mm. The raw data were transferred automatically via Ethernet to a workstation (ADW 4.2; GE Medical Systems) in a 512× 512-pixel format. The oblique angles for the multiplanar reformatting (MPR) images were selected to follow the course of the main pancreatic duct near the cystic lesion on the axial images. The use of interactive oblique views facilitated selection of the appropriate angles. To generate curved planar reformatting (CPR) images, the operator designated a curved line along the long axis of the pancreas by scrolling and reviewing a stack of axial images. Multiple images were generated parallel to this curved plane.

MRCP technique

MR imaging of the pancreas and MRCP were performed with a 1.5-T system (MAGNETOM Sym-

phony Maestro Class; Siemens, Erlangen, Germany) using a phased-array body coil. T1-weighted gradient–recalled echo images were obtained through the pancreas before and after fat saturation (repetition time msec/echo time msec, 180/2.1; flip angle, 80°; number of signals acquired, 1; matrix, 192×256; section thickness, 7.00 mm). T2-weighted MRCP was performed using a single-shot rapid acquisition with relaxation enhancement (RARE) and three-dimensional turbo spin echo (3D-TSE) sequence (TR=1590 msec, TE=761 msec) with 1.8-mm section thickness, resulting in a total of 61 sections. All images were post-processed using both maximum intensity projection (MIP) and MPR techniques, including coronal, coronal oblique, and transverse planes. No intravenous contrast material was administered for MRCP.

EUS technique

Endoscopes with 7.5-12-MHz probe radial sector scan transducers (GF-UMQ-200; Olympus, Tokyo, Japan) were used. The echo probe was routinely covered with a water-filled balloon to allow adequate transmission of ultrasound and to improve image quality. The echo endoscope was introduced into the stomach and advanced into the second portion of the duodenum. Tumors were scanned with a water-filled balloon to assess tumor features.

Image analysis

MDCT and MRCP imaging findings were evaluated by the consensus of two radiologists who had 13 and 25 years of experience reading abdominal images, respectively. The readers were aware of the diagnosis of branch duct IPMNs of the pancreas but were blinded to the histopathologic findings. In addition, EUS reports from gastroenterologists were analyzed retrospectively.

Imaging criteria for diagnosing malignancy

Malignancy was diagnosed by MDCT or MRCP when at least one of the following was detected: thickened irregular walls/septa in which enhancement can be demonstrated, or a solid mass within the dilated branch pancreatic duct. A small intramural nodule measuring less than 10 mm associated with enhancing soft-tissue components adjacent to the walls/septa was defined as thickened irregular walls/septa (Fig. 1A). On the other hand, a large intramural nodule measuring 10 mm or larger, and associated with enhancing soft-tissue components adjacent to the wall or septa, was defined as a solid mass (Fig. 1B). Findings of solid mass and thickened irregular walls/septa were evaluated with portal or venous phase axial images, interactive MPR, and source images. Additionally, the maximum diameter of MPD and cyst size were recorded for each patient. The maximum diameters of the MPD and cyst size were measured on the MPR or CPR image and the MIP image. The diameter and size of nodules were measured at the workstation with electronic calipers. Malignancy was diagnosed when

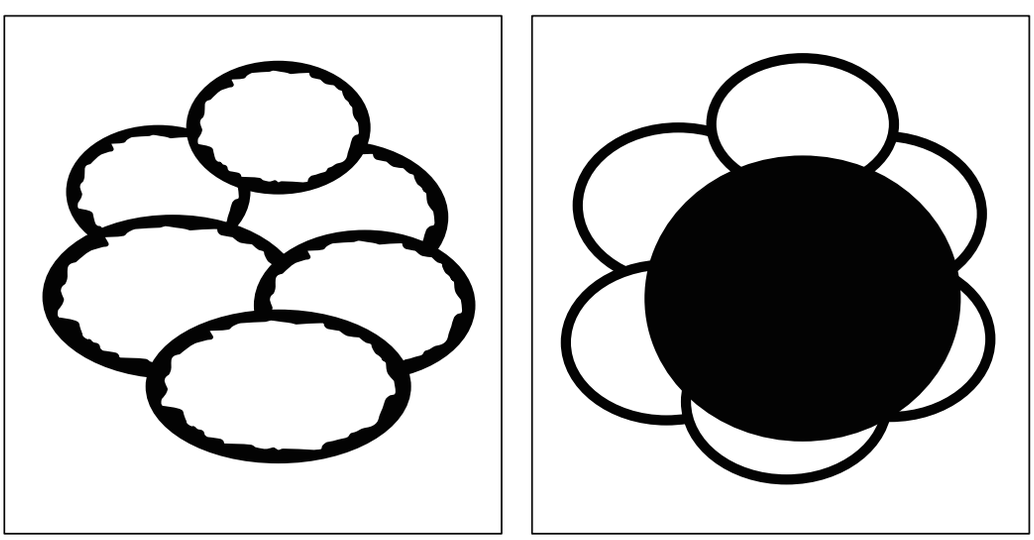

Fig. 1. Schematic diagrams of cystic lesions on MDCT and MRCP.
A. "Thickened irregular walls/septa" were defined as a wall or septum with adjacent enhancing soft-tissue components.
B. "A solid mass" was defined as an intramural nodule measuring 10 mm or larger in the cystic lesion.

either an intramural nodule or solid mass was detected using EUS. Intramural nodules detected by EUS were defined as hyperechoic nodules lining the walls.

Histopathologic analysis

A gastrointestinal pathologist with more than 8 years of experience reviewed each pathologic specimen. Tumors were classified into three histologic subtypes by microscopy as follows: adenoma, borderline lesion, or carcinoma. Carcinoma in situ and invasive carcinoma were grouped together as carcinoma. Classifications were made in accordance with World Health Organization (WHO) definitions [7].

Statistical analysis

The Bonferroni multiple comparison test was used to assess correlations between continuous variables, including the diameter of the main pancreatic duct and the lesion size. Differences between ordinal variables were evaluated using the Wilcoxon-Mann-Whitney test. A p-value of less than 0.05 was considered statistically significant. Statistical analysis was performed with SPSS for Windows release 12.0.0 (SPSS, Chicago, IL, USA).

RESULTS

Surgical results

Lesions were resected by pancreaticoduodenectomy in 7 patients, pylorus-preserving pancreaticoduodenectomy in 9 patients, distal pancreatectomy and splenectomy in 6 patients, partial resection in 2 pa-

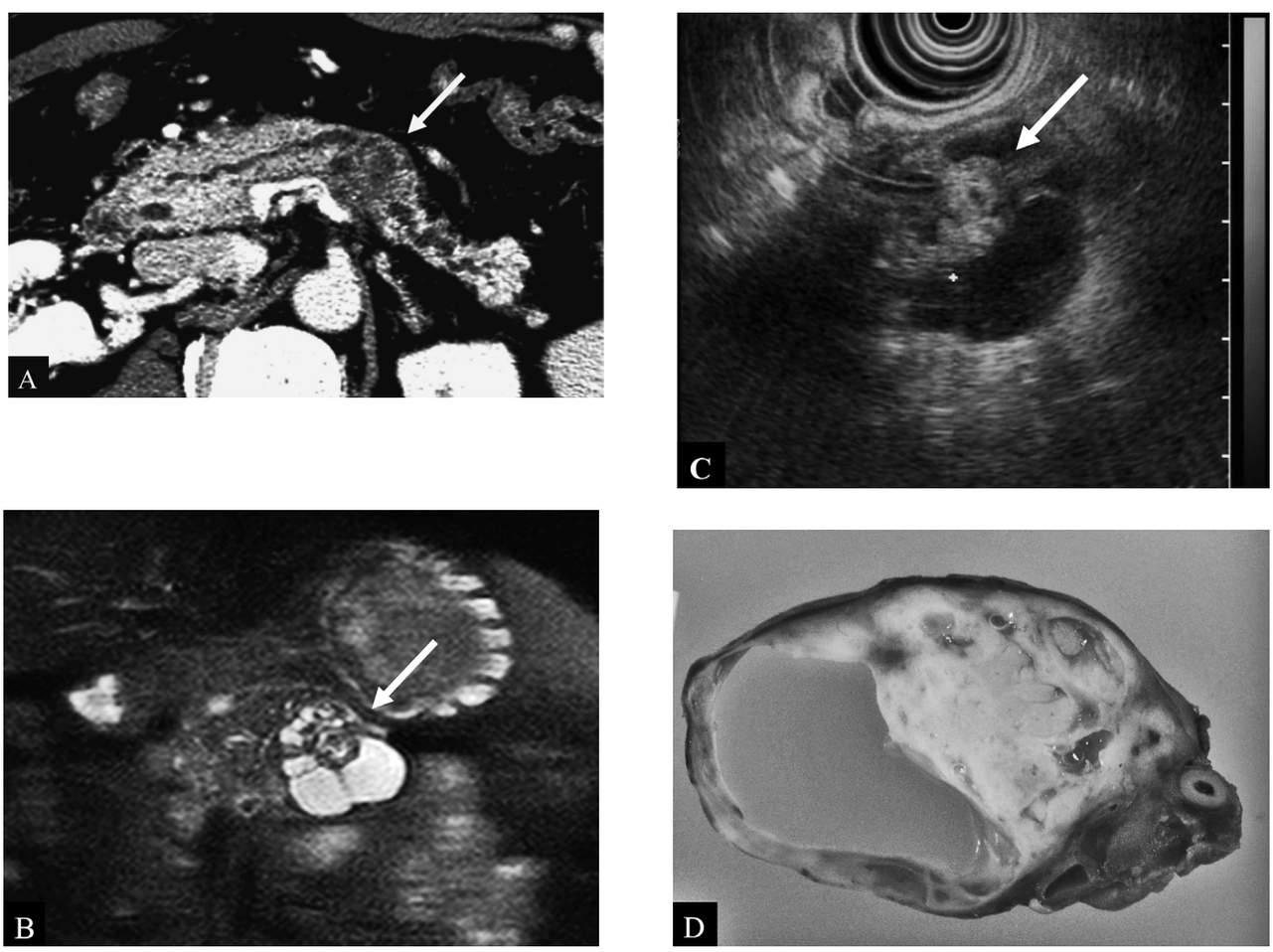

Fig. 2. A 47-year-old man with intraductal papillary mucinous neoplasm (IPMN) with invasive carcinoma.
A. Curved planar reformation demonstrates a heterogeneous hypoattenuating solid mass measuring 30 mm in diameter in the dilated branch duct (arrow) of the pancreatic body. The main pancreatic duct is diffusely dilated.
B. Source MRCP image shows a solid mass (arrow) in the multilocular cystic lesion.
C. EUS shows a solid mass within a cystically dilated branch duct.
D. Photograph of the resected specimen shows a solid mass in the cystically dilated branch duct. Microscopic examination reveals intraductal papillary adenocarcinoma. The papillary adenocarcinoma spread through the periductal tissue into the pancreatic body.

TABLE 1.
Correlation between presence of thickened walls/septa or solid mass and histology on MDCT

	Adenoma	Borderline	Carcinoma	*P*-value
thickened walls/septa				
presence	0	3	3	0.019
absence	13	1	5	
solid mass				
presence	0	0	5	0.001
absence	13	4	3	

Data are numbers of patients.

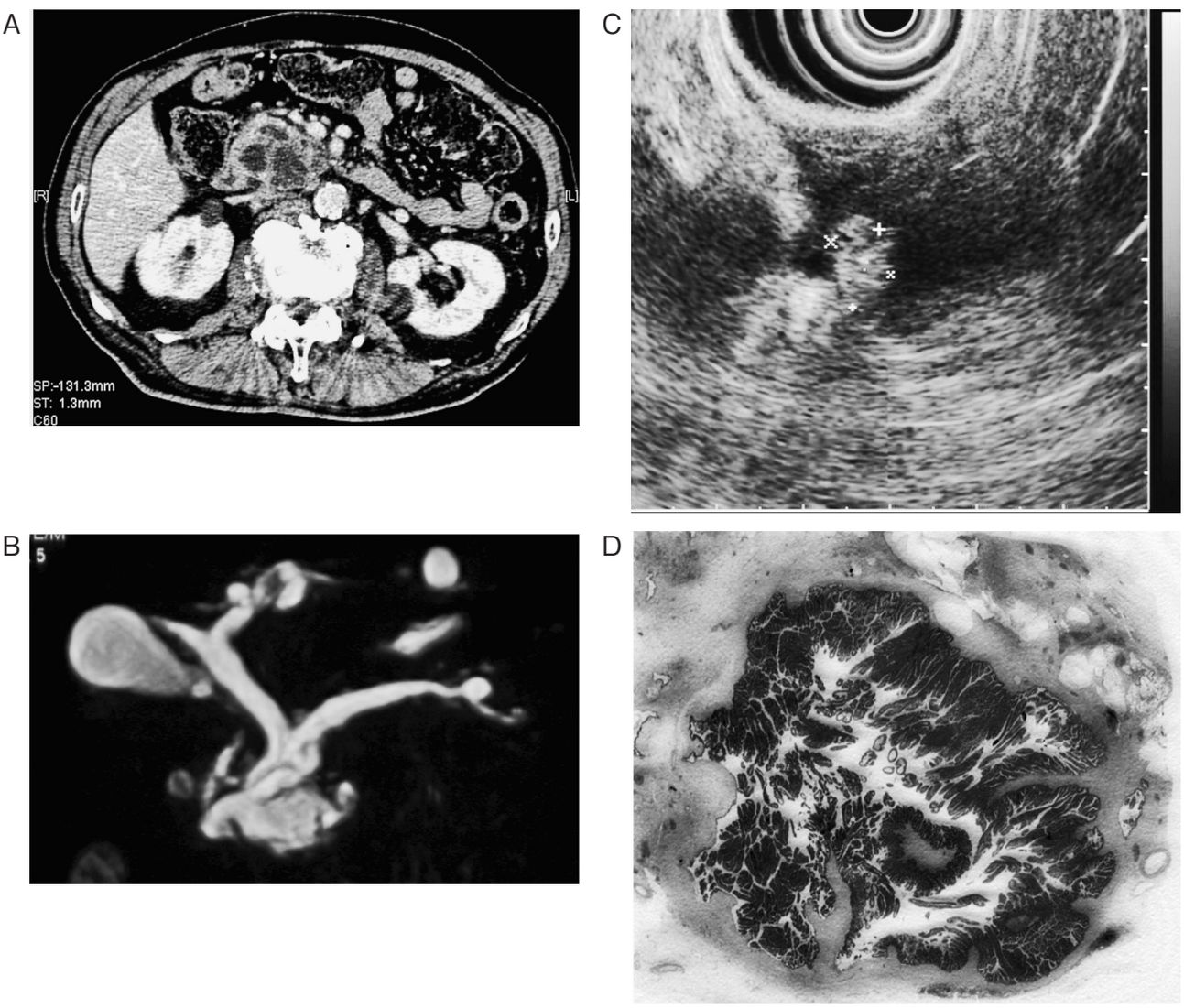

Fig. 3. A 78-year-old man with intraductal papillary mucinous neoplasm (IPMN) with minimally invasive carcinoma.
A. Axial CT image shows a cystic tumor measuring 45 mm in diameter with thickened irregular walls/septa in the pancreas head.
B. MRCP image shows multiseptated cystic mass with upstream diffuse dilatation of the main pancreatic duct. The cystic mass had low signal intensity septa within the lesion, but did not show thickened irregular septa.
C. EUS shows an intramural nodule as a hyperechoic lesion measuring 8 mm in diameter within the cystic mass.
D. Microscopic examination reveals intraductal papillary adenocarcinoma of the tall columnar epithelium with severe atypia in the pancreatic duct. This figure is reproduced from Reference 6 (Arikawa et al.) with permission from the journal.

tients, and total pancreatectomy in 1 patient.

Pathologic results

Diagnosis of branch duct type IPMN was confirmed by histologic examination and classified as follows: 13 samples (52%) as adenoma, 8 samples (32%) as carcinoma, and 4 samples (16%) as borderline. Of the 8 patients with carcinoma, 5 patients were diagnosed with invasive carcinoma and 3 patients were diagnosed with small or microscopic foci of invasive carcinoma.

Imaging examinations

MDCT and MRCP imaging were performed on all patients without complications. EUS was performed in 19 patients; EUS was unsuccessful in 3 patients because of previous distal gastrectomy with Billroth Ⅱ anastomosis.

Correlation between histopathology and imaging findings on MDCT

A solid mass was detected in 5 of 8 carcinomas (Figs. 2A, D), but not in adenomas or borderline lesions. Thickened irregular walls/septa were detected by MDCT in 3 of 8 carcinomas (Figs. 3A, D) and in 3 of 4 borderline lesions, but were not detected in adenomas (Figs. 4A, B, D). A significant correlation was found between these MDCT features and malignancy (Table 1).

Correlation between histopathology and imaging findings on MRCP

A solid mass was detected in 5 of 8 carcinomas (Fig. 2B), in none of the borderline lesions, and in 1 of 13 adenomas-although this case was determined to be a false positive (i.e., pancreatic calcification). Thickened irregular walls/septa were detected in 1 of 8 car-

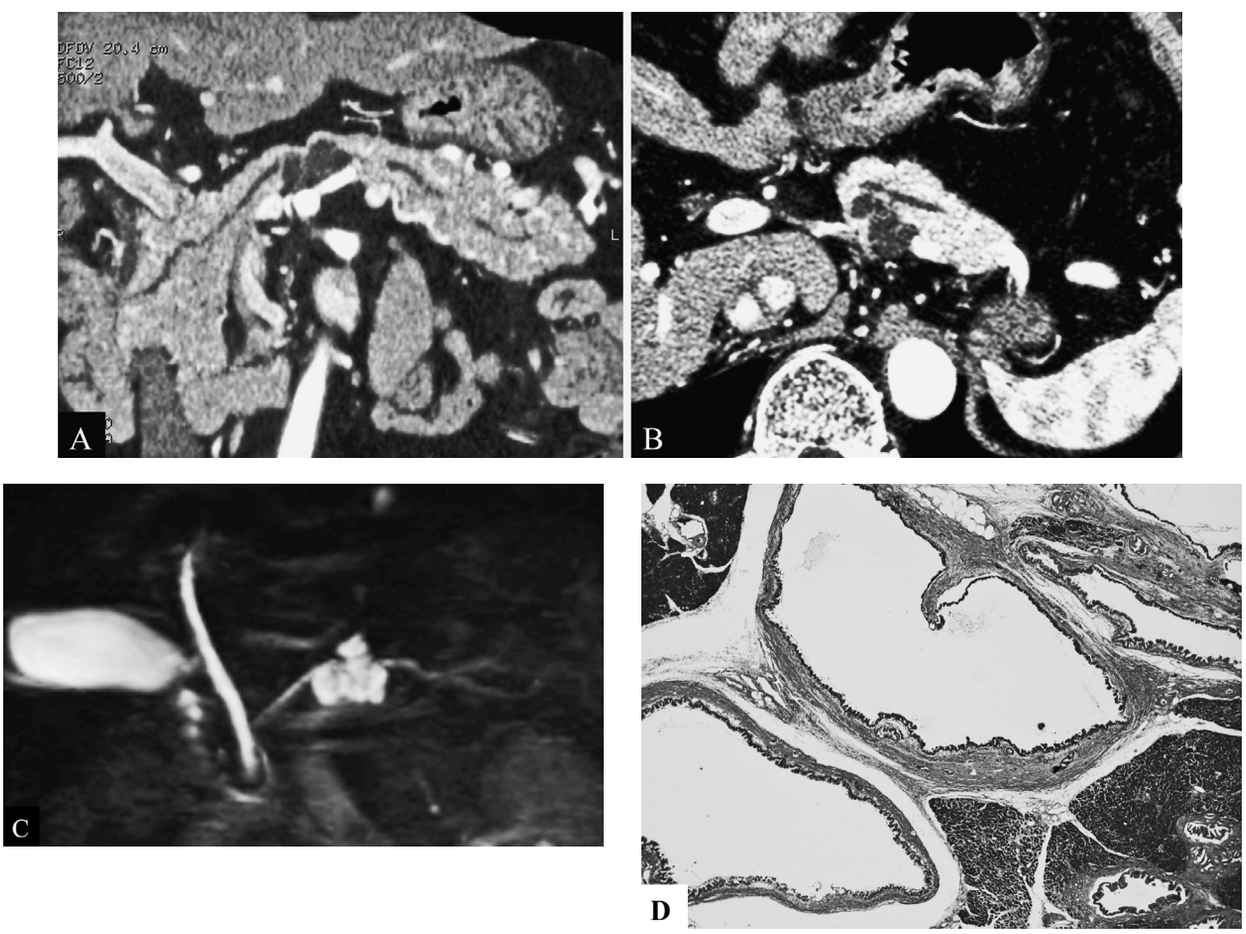

Fig. 4. A 67-year-old man with intraductal papillary mucinous neoplasm (IPMN) with adenoma.
A. Curved planar reformation and B. axial contrast enhanced CT image shows the cystic lesion measuring 22 mm in diameter with thin septa in the pancreatic body. The main pancreatic duct is minimally dilated.
C. MRCP image shows multiseptated cystic mass with thin septa.
D. Microscopic examination reveals the presence of papillae with low-grade dysplasia of the epithelium. The tumor was diagnosed as intraductal papillary adenoma with mild dysplasia.

TABLE 2.
Correlation between presence of thickened walls/septa or solid mass and histology on MRCP

	Adenoma	Borderline	Carcinoma	*P*-value
thickened walls/septa				
presence	0	1	1	0.46
absence	13	3	7	
solid mass				
presence	1†	0	5	0.008
absence	12	4	3	

Data are numbers of patients. † Pancreatolith

TABLE 3.
Correlation between presence of intramural nodule or solid mass and histology on EUS

	Adenoma	Borderline	Carcinoma	*P*-value
intramural nodule				
presence	5	0	1	0.121
absence	5	3	5	
solid mass				
presence	0	1	4	0.0009
absence	10	2	2	

Data are numbers of patients.

cinomas (Fig. 3B) and in 1 of 4 borderline lesions, but were not detected in adenomas (Fig. 4C). A significant correlation was found between MRCP detection of a solid mass and malignancy, but no significant correlation was found between the detection of thickened irregular walls or septa and malignancy (Table 2).

Correlation between histopathology and imaging findings on EUS

A solid mass was found in 4 of 6 carcinomas (Fig. 2C), in 1 of 3 borderline lesions, but not in adenomas. An intramural nodule was detected in 5 of 10 adenomas, but in none of the 3 borderline lesions, and 1 of 6 carcinomas (Fig. 3C). A significant correlation was found between EUS detection of a solid mass and malignancy, but no significant correlation was found between the detection of an intramural nodule and malignancy (Table 3).

Correlation between histopathology and the maximum diameter of the MPD or cyst size

The relationship between histopathologic findings and the mean maximum diameter of the MPD detected by MDCT and MRCP was examined. The mean maximum diameter of MPD for adenoma, borderline lesion, and carcinoma was 6.2±4.9 mm, 6.2±1.5 mm, and 6.6±3.5 mm by MDCT, respectively; and 6.5±1.9 mm, 6.7±3.6 mm, and 6.8±5.5 mm by MRCP, respectively. The values for malignant tumors tended to be larger, but no significant correlation was found between the average maximum diameter of the MPD and malignancy.

The relationship between histopathologic findings and cyst size detected by MDCT and MRCP was also examined. The mean size of adenoma, borderline lesion, carcinoma was 29.0±10.6 mm, 31.9±7.5 mm, and 42.5±21.1 mm by MDCT, respectively; and 29.7 ±10.6 mm, 31.3±8.5 mm, and 42.2±20.7 mm by MRCP, respectively. The values for malignancy tumors tended to be larger, but no significant correlation was found between cyst size and malignancy.

DISCUSSION

Several imaging criteria for branch duct IPMNs of the pancreas have been reported to differentiate malignant lesions from benign lesions. However, the diagnostic significance of these criteria and diagnosis methods have not been established and are controversial. Recently, international guidelines for the management of IPMNs were proposed by the International Association of Pancreatology [8]. These guidelines

recommend that presence of intramural nodules, cyst size >30 mm, and dilation of the MPD (>6 mm) be used as indications for resection. Moreover, the guidelines recommend using MDCT or MRCP to assess the size of the lesion and the MPD diameter. In addition, the guidelines recommend EUS for intramural nodules. EUS may be the most sensitive method for visualizing small architectural features like intramural nodules [9,10]; however, this technique has some drawbacks. EUS is an invasive procedure, dependent on technical skills of the operator, and does not provide the surgeon with a visual "road map" to reference for preoperative planning. Thus, minimally invasive or noninvasive imaging methods for diagnostic and preoperative examinations would be advantageous for patients and surgeons. Fukukura et al. [11] reported that papillary proliferation (≥3 mm) was detected equally well by helical CT and MRCP. However, in our experience, the CT and MRCP techniques often detect only a thickened septum and have difficulty detecting intramural nodules due to the limited spatial resolution of the typically small, flat tumor. Therefore, we compared the ability of the following the imaging criteria to diagnose malignancy of branch duct IPMNs of the pancreas: detection of an intramural nodule (<10 mm diameter) or a solid mass (≥10 mm diameter) by EUS, and detection of a solid mass or thickened irregular walls/septa by MDCT or MRCP.

In our study, the presence of a solid mass correlated well with malignancy for all imaging methods. Previous studies have reported that the presence of a solid mass is predictive of malignancy using several types of imaging, including CT [12-14], MRI [15], and EUS [9,16]. Our findings support these studies. We did not see differences in detection rate based on different modalities. In addition, the presence of thickened irregular walls/septa on MDCT also correlated well with malignancy. Procacci et al. [17] reported that in malignant lesions, the wall and septa appear irregular and thick, indicating intramural nodules, whereas both the wall and septa are regular and thin in benign lesions. Carbognin et al. [18] reported that the presence of a thick wall by CT and MR imaging is strongly suggestive of malignancy. In the present study, however, the presence of thickened irregular walls/septa on MRCP did not correlate well with the presence of malignancy. Neither MRCP nor MDCT can visualize fine structures of cystic lesions due to limited spatial resolution. Pathologically, thickened irregular walls/septa mainly result from fibrosis of pancreatic parenchyma due to obstructive chronic pancreatitis and large papillary protrusions lining the dilated branch duct wall. Thus, it is prudent to suspect malignancy when MDCT, but not MRCP, detects thickened irregular walls/septa in which enhancement can be demonstrated. Conversely, MDCT and MRCP detection of hairline-thin septa, or minimal but smooth thickening of walls/septa, suggests benign lesions. The presence of intramural nodules on EUS did not correlate well with malignancy. Kobayashi et al. [16] reported that none of the patients with intramural nodules less than 10 mm visualized by EUS had developed invasive carcinoma at resection. Loftus et al. [19] reported that histologic diagnosis of malignancy depends on the nuclear appearance of the intramural nodule, rather than its presence alone. The presence and size of intramural nodules have previously been considered significant findings in diagnosing malignancy. However, in the present study, nodules less than 10 mm were visualized by EUS in 50% (5/10) of adenomas, and were not significantly different. In contrast, the presence of thickened irregular walls/septa was not detected in any adenoma by MDCT or MRCP. In MDCT, this finding was observed significantly in malignancies and borderline malignancies. These results suggest that evaluating the presence of thickened irregular walls/septa by MDCT, as well as the presence of intramural nodules, is important in diagnosing malignancy.

Large tumor size and marked dilation of the MPD in branch duct IPMNs have also been reported to be associated with malignancy[14,20-25], but this conclusion was not confirmed by other studies [4,18,24, 26-28]. In the present study, both maximal MPD diameter and size of the entire cystic lesion were larger in malignant than in benign lesions, but this difference was not statistically significant. This is due to the massive production of mucin characteristic of pancreatic IPMNs, which leads to increased cyst size and a dilated MPD. Thus, increased cyst size and dilated MPD were not necessarily suggestive of malignancy.

There are several limitations to our study. First, it is limited by the small patient sample size; however, all cases were well documented with detailed surgical and pathological findings. Second, while decisions on MDCT and MRCP findings were based on the consensus of two radiologists, we did not evaluate interobserver agreement. Third, criteria for determining malignancy were not the same for all imaging methods. Thickened irregular walls/septa were not evaluated by EUS because this finding was not included in past EUS reports, which were analyzed retrospectively in the present study. Fourth, due to the small sample size and limited number of findings examined, we did not

determine using multivariable analysis whether or not the presence of a solid mass or thickened irregular walls/septa on MDCT is an independent risk factor.

In conclusion, MDCT was useful for diagnosis of branch duct IPMNs of the pancreas. In particular, the presence of a solid mass and thickened irregular walls/septa on MDCT, but not on MRCP or EUS, correlated well with malignancy.

REFERENCES

1. Yamada M, Kozuka S, Yamao K, Nakazawa S, Naitoh Y et al. Mucin-producing tumor of the pancreas. Cancer 1991; 68:159-168.
2. Kobari M, Egawa S, Shibuya K, Shimamura H, Sunamura M et al. Intraductal papillary mucinous tumors of the pancreas comprise 2 clinical subtypes: differences in clinical characteristics and surgical management. Arch Surg 1999; 134:1131-1136.
3. Terris B, Ponsot P, Paye F, Hammel P, Sauvanet A et al. Intraductal papillary mucinous tumors of the pancreas confined to secondary ducts show less aggressive pathologic features as compared with those involving the main pancreatic duct. Am J Surg Pathol 2000; 24:1372-1377.
4. Irie H, Yoshimitsu K, Aibe H, Tajima T, Nishie A et al. Natural history of pancreatic intraductal papillary mucinous tumor of branch duct type: follow-up study by magnetic resonance cholangiopancreatography. J Comput Assist Tomogr 2004; 28:117-122.
5. Sai JK, Suyama M, Kubokawa Y, Yamanaka K, Tadokoro H et al. Managemant of branch duct-type intraductal papillary mucinous tumor of the pancreas based on magnetic resonance imaging. Abdom Imaging 2003; 28:694-699.
6. Arikawa S, Uchida M, Shinagawa M, Uozumi J, Hayabuchi N et al. The role of multi-detector-row computed tomograph in the diagnosis of intraductal papillary-mucinous tumors of the pancreas in comparison to endoscopic retrograde pancreatography, endoscopic ultrasonography, magnetic resonance cholangiopancreatography. Nippon Shokakibyo Gakkai Zasshi 2007; 104:373-380. (in Japanese)
7. Longnecker DS, Adler G, Hruban RH, and Kloppel G. Intraductal papillary mucinous neoplasms of the pancreas. In: WHO classification of tumors of the digestive system, ed. World Health Organization, Geneva, Switzerland, pp 237-240, 2000.
8. Tanaka M, Chari S, Adsay V, Fernandez-Del Castillo C, Falconi M et al. International Consensus Guidelines for Management of Intraductal Papillary Mucinous Neoplasms and Mucinous Cystic Neoplasms of the Pancreas. Pancreatology 2005; 6:17-32.
9. Kubo H, Chijiiwa Y, Akahoshi K, Hamada S, Harada N et al. Intraductal papillary-mucinous tumors of the pancreas: differential diagnosis between benign and malignant tumors by endoscopic ultrasonography. Am J Gastroenterol 2001; 96:1429-1434.
10. Yamao K, Ohashi K, Nakamura T, Suzuki T, Watanabe Y et al. Evaluation of Various Imaging Methods in the Differential Diagnosis of Intraductal Papillary-Mucinous Tumor (IPMT) of the Pancreas. Hepato-Gastroenterology 2001; 48:962-966.
11. Fukukura Y, Fujiyoshi F, Hamada H, Takao S, Aikou T et al. Intraductal papillary mucinous tumors of the pancreas. Comparison of helical CT and MR imaging. Acta Radiol 2003; 44:464-471.
12. Yamada Y, Mori H, Matsumoto S, Kamei N, Hongo N et al. Invasive carcinomas derived from intraductal papillary mucinous neoplasms of the pancreas: a long-term follow-up assessment with CT imaging. J Comput Assist Tomogr 2006; 30:885-890.
13. Kawamoto S, Lawler LP, Horton KM, Eng J, Hruban RH et al. MDCT of intraductal papillary mucinous neoplasm of the pancreas: evaluation of features predictive of invasive carcinoma. AJR Am J Roentgenol 2006; 186:687-695.
14. Taouli B, Vilgrain V, Vullierme MP, Terris B, Denys A et al. Intraductal papillary mucinous tumors of the pancreas: helical CT with histopathologic correlation. Radiology 2000; 217:757-764.
15. Pilleul F, Rochette A, Partensky C, Scoazec J-Y, Bernard P et al. Preoperative Evaluation of Intraductal Papillary Mucinous Tumors Performed by Pancreatic Magnetic Resonance Imaging and Correlated With Surgical and Histopathologic Findings. J Magn Reson Imaging 2005; 21:237-244.
16. Kobayashi G, Fujita N, Noda Y, Ito K, Horaguchi J et al. Mode of progression of intraductal papillary-mucinous tumor of the pancreas: analysis of patients with follow-up by EUS. J Gastroenterol 2005; 40:744-751.
17. Procacci C, Megibow AJ, Carbognin G, Suzuki T, Watanabe Y et al. Intraductal Papillary Mucinous Tumor of the Pancreas: A Pictorial Essay. RadioGraphics 1999; 19:1447-1463.
18. Carbognin G, Zamboni G, Pinali L, Chiara ED, Girardi V et al. Branch duct IPMTs: value of cross-sectional imaging in the assessment of biological behavior and follow-up. Abdom Imaging 2006; 31:320-325.
19. Loftus EV, Jr., Olivares-Pakzad BA, Batts KP, Adkins MC, Stephens DH et al. Intraductal papillary-mucinous tumors of the pancreas: clinicopathologic features, outcome, and nomenclature. Members of the Pancreas Clinic, and Pancreatic Surgeons of Mayo Clinic. Gastroenterology 1996; 110:1909-1918.
20. Sugiyama M, Izumisato Y, Abe N, Masaki T, Mori T et al. Predictive factors for malignancy in intraductal papillary-mucinous tumours of the pancreas. Br J Surg 2003; 90:1244-1249.
21. Kimura W, Sasahira N, Yoshikawa T, Muto T, and Makuuchi M. Duct-ectatic type of mucin producing tumor of the pancreas--new concept of pancreatic neoplasia. Hepatogastroenterology 1996; 43:692-709.
22. Uehara H, Nakaizumi A, Iishi H, Tatsuta M, Kitamra T et al. Cytologic examination of pancreatic juice for differential diagnosis of benign and malignant mucin-producing tumors of the pancreas. Cancer 1994; 74:826-833.
23. Baba T, Yamaguchi T, Ishihara T, Kobayashi A, Oshima T et al. Distinguishing benign from malignant intraductal papillary mucinous tumors of the pancreas by imaging techniques. Pancreas 2004; 29:212-217.

24. Sahani DV, Kadavigere R, Blake M, Fernandez-Del Castillo C, Lauwers GY et al. Intraductal papillary mucinous neoplasm of pancreas: multi-detector row CT with 2D curved reformations--correlation with MRCP. Radiology 2006; 238:560-569.
25. Sugiyama M, Atomi Y, and Kuroda A. Two types of mucin-producing cystic tumors of the pancreas: diagnosis and treatment. Surgery 1997; 122:617-625.
26. Fukukura Y, Fujiyoshi F, Sasaki M, Inoue H, Yonezawa S et al. Intraductal papillary mucinous tumors of the pancreas: thin-section helical CT findings. AJR Am J Roentgenol 2000; 174:441-417.
27. Schmidt CM, White PB, Waters JA, Yiannoutsos CT, Cummings OW et al. Intraductal papillary mucinous neoplasms: predictors of malignant and invasive pathology. Ann Surg 2007; 246:644-651.
28. Azar C, Van de Stadt J, Rickaert F, Deviere M, Baize M et al. Intraductal papillary mucinous tumours of the pancreas. Clinical and therapeutic issues in 32 patients. Gut 1996; 39:457-464.

Original Contribution

Kurume Medical Journal, 57, 101-108, 2010

"Hybrid Exercise" Prevents Muscle Atrophy in Association with a Distinct Gene Expression Pattern

TORU MATSUGAKI*, NAOTO SHIBA*,**, SHOHEI KOHNO†, TAKESHI NIKAWA†, KATSUYA HIRASAKA†, YUUSHI OKUMURA†, KAZUMI ISHIDOH‡, TAKASHI SOEJIMA*, KAZUHIRO YOSHIMITSU* AND KENSEI NAGATA*

**Department of Orthopedics, Kurume University School of Medicine, Kurume 830-0011,*
***Rehabilitation Center, Kurume University Medical Center, Kurume 839-0863,*
†Department of Nutritional Physiology, Institute of Health Biosciences,
The University of Tokushima Graduate School, Tokushima 770-8503 and
‡Institute for Health Sciences, Tokushima-Bunri University, Tokushima 770-8514, Japan

Received 27 August 2010, accepted 4 October 2010

Edited by KOJI TOYOMASU

Summary: "Hybrid exercise" utilizing combined electrical stimulation and voluntary muscle contraction has been developed as a muscle exercise method. Although our previous studies have confirmed the effectiveness of the procedure, the mechanisms of its efficacy still remain unclear. In the present study, we identified genes that are specifically expressed in disused muscles, using the semitendinosus muscle from patients who underwent anterior cruciate ligament (ACL) reconstruction. Preoperative exercise was performed by four ACL-injured patients, who were subjected either to hybrid exercise (n=2), electrical stimulation (n=1), or no electrical stimulation (n=1), in addition to standard weight training for 4 weeks. Cross-sectional area (CSA) of the semitendinosus muscle was measured before and after the exercise by magnetic resonance imaging (MRI). A piece of the semitendinosus muscle was isolated during the surgery, and comprehensive analysis of the gene expression in this sample was performed using DNA microarray analysis. CSA increased in size by 4.2 and 14.7%, respectively, after hybrid exercise, and by 1.4% after electrical stimulation. However it shrunk by 7.7% without electrical stimulation. DNA microarray analysis revealed that hybrid exercise was more effective at stimulating the expression of signal transduction-, transcription- and cytoskeleton-related genes in semitendinosus muscles than electrical stimulation alone. In particular, gene ontology analysis revealed that hybrid exercise induced significantly higher expression of eukaryotic translation initiation factor 5A (EIFSA), peroxisomal biogenesis factor 6 (PEX6) and histone cluster 1 H4 (HIST1H4), compared with electrical stimulation alone. The expression of signal transduction-, transcription- and cytoskeleton-related genes may play an important role in muscle bulk increasing mechanisms in hybrid exercise.

Key words anterior cruciate ligament-injured patients, neuromuscular electrical stimulation, gene expression, muscle strengthening exercise, disuse-induced muscle atrophy

Corresponding author: Naoto Shiba, M.D. and Ph.D., Department of Orthopedics, Kurume University School of Medicine, 67 Asahi-machi, Kurume 830-0011, Japan. Tel: 0942-31-7568 Fax: 0942-35-0709 E-mail: nshiba@med.kurume-u.ac.jp

Abbreviations: ACL, anterior cruciate ligament; AM, adductor muscles; BFL, biceps femoris long head; BFS, biceps femoris short head; CSA, cross-sectional area; EIF5A, eukaryotic translation initiation factor 5A; FHOD3, formin homology 2 domain containing 3; GAPDH, glyceraldehyde-3-phosphate dehydrogenase; GM, gracilis muscle; GO, gene ontology; HIST1H4, histone cluster 1 H4; MRI, magnetic resonance imaging; PEX6, peroxisomal biogenesis factor 6; RF, rectus femoris; RT-PCR, reverse transcription and polymerase chain reaction; SaM, sartorius muscle; SM, semimembranosus muscle; ST, semitendinous muscle; VI, vastus intermedius; VL, vastus lateralis; VM, vastus medialis.

INTRODUCTION

We recently developed a "hybrid exercise" technique that resists the motion of a volitionally contracting muscle by means of a force generated by an electrically stimulated antagonist (Fig. 1) [1-4]. This technique utilizes electrically stimulated eccentric contractions and concentric volitional contractions involving reciprocal limb movements, and requires minimal external stabilization as compared with conventional weight training. Matsuse et al. [1] have shown that such hybrid exercise increased the extension torque of the elbow joint by about 30% and the cross-sectional areas (CSA) of the proximal upper extremity muscles by about 15% over a 12-week period. In addition, Iwasaki et al. [2] demonstrated that 6 weeks of hybrid exercise effectively increased the extension torque of the knee joint by 19-33%. Takano et al. also demonstrated that 12 weeks of hybrid exercise increased the knee extension torque by 39% and the CSA of quadriceps muscle by 9% in elderly subjects [3]. However, the mechanism by which hybrid exercise achieves these increases in muscular strength and bulk are still unknown.

Muscle atrophy occurs as a consequence of denervation, injury, joint immobilization, bed rest, glucocorticoid treatment, sepsis, cancer, and aging [5]. Unfortunately, there is no effective treatment for muscle atrophy. The maintenance of muscle mass is controlled by a balance between protein synthesis and protein degradation pathways, which is thought to shift toward protein degradation during atrophy [5]. Recently, a signaling pathway that increases protein synthesis was shown to promote muscle hypertrophy, thereby overcoming muscle atrophy [6,7]. This finding led us to examine the effects of hybrid exercise on muscle power and muscle bulk in disuse-induced atrophic muscle at the genetic level. In the present study, we examined the gene expression profile in atrophied muscles of patients who underwent hybrid exercise.

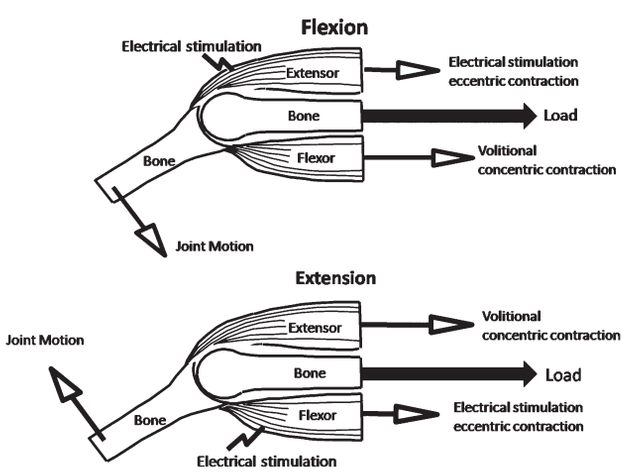

Fig. 1. Schematic model of hybrid exercise.
Hybrid exercise resists utilizes electrically stimulated eccentric contractions and concentric volitional contractions with reciprocal limb movements. Both the volitionally activated agonist and the electrically stimulated antagonist contract during joint motion. The result is that both muscles are trained and that a longitudinal compressive load is placed on the bone.

MATERIALS AND METHODS

Subjects and exercise procedure

Four patients with anterior cruciate ligament (ACL) injuries were recruited for this study. Their average age was 17.8 years old (range 15-24). They were all scheduled to undergo ACL reconstruction surgery, and were subjected either to hybrid exercise (n=2), electrical stimulation (control 1; n=1) or no electrical stimulation (control 2; n=1), as described below. The subjects exercised three times a week for four weeks immediately before the ACL reconstruction surgery, and the exercises were done only on the affected side. Patients in all three groups were routinely subjected to half squat and calf raise exercise as standard weight training. One section of the standard weight training consisted of 5 sets of 20 repetitions.

All protocols used in this study were approved by the Ethics Committee of Kurume University (approved NO.06009). Following approval, informed consent was obtained from the subjects who had reviewed the goals of the study and agreed to participate. For minor subjects, approval was also obtained from their legal guardian.

Hybrid exercise

The subjects in this group were made to sit in a chair. The hamstring muscle was then electrically stimulated during volitional knee extension, and the quadriceps muscle was stimulated during volitional knee flexion. Each session included 10 sets of 10 reciprocal 3-sec (30°/sec) knee extensions and flexions. The sets were separated by 1-min rest intervals, and an exercise session required 19 min to complete. The electrical stimulation device has been described previously [8]. The stimulation waveform used in this study was similar in some ways to that used in "Russian stimulation [9]," and consisted of a 5,000 Hz carrier frequency modulated at 20 Hz (2.4 ms on, 47.6 ms off) to deliver

a rectangular biphasic pulse [3,8]. The stimulation intensities were set at 70% of the maximum comfortable intensity, which was determined by increasing the stimulation voltage until the subjects reported any discomfort, for the quadriceps muscle, and at 80% of that for the hamstring muscle [3].

Electrical stimulation

The subject was instructed to relax and not to attempt a volitional muscle contraction with the knee immobilized in a brace at full extension. The wave form, frequency, stimulation intensity and number of repetitions were the same as for the subject receiving hybrid exercise.

Measurement of cross-sectional areas of semitendinosus muscles

CSA of the semitendinosus muscle which would be collected for subsequent DNA microarray analyses was measured by means of magnetic resonance imaging: MRI (Signa LX 1.5 Tesla; GE Healthcare, New York, NY, USA) (Fig. 2). Consecutive transaxial T1-weighted images (spin-echo; TR=720 ms, TE=0.7 ms, matrix size=384×256, FOV=48 cm×36 cm, slice thickness=8 mm, inter slice gap=2 mm) were obtained. The subjects were scanned in a supine position with the knee fully extended and the ankles fixed by an apparatus which was designed especially for this study. The number of transaxial images obtained for each subject was 30. From these images, the image that corresponded to the middle region along the length of the thigh was chosen. CSAs of the semitendinosus muscle were all analyzed by a blinded assessor using NIH Image software (Image J, version 1.410; NIH, Bethesda, MD, USA) [3].

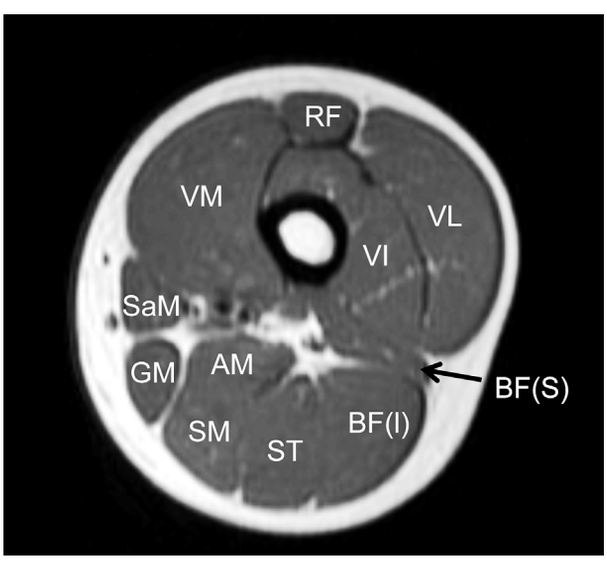

Fig. 2. Cross sectional area of thigh muscles.
The semitendinous muscles which were to be collected for subsequent DNA microarray analyses were measured in an MRI. VL, vastus lateralis; VM, vastus medialis; VI, vastus intermedius; RF, rectus femoris; BFL, biceps femoris long head; BFS, biceps femoris short head; ST, semitendinous muscle; SM, semimembranosus muscle; AM, Adductor muscles, SaM, Sartorius muscle; GM, Gracilis muscle.

Sampling of human skeletal muscle and RNA isolation

All patients in this study underwent ACL reconstruction surgery after training with hybrid exercise, electrical stimulation alone, or without electrical stimulation, as described above. In the ACL reconstruction surgery, the semitendinosus tendon must be prepared as a self-graft. After obtaining informed consent from all patients, a small amount of muscle attached to this tendon, which was redundant for the graft, was collected for the present study. The samples were immediately frozen in liquid nitrogen and stored at −80°C until the analyses.

Total RNA was isolated from the semitendinosus-muscles using RNA isolation solution (Nippon Gene, Tokyo, Japan) according to the manufacturer's instructions. The RNA pellets were resuspended in diethyl pyrocarbonate1-treated water. The quantity and quality of RNA obtained were estimated by an Agilent 2100 Bioanalyzer (Agilent Technologies, Santa Clara, CA, USA).

DNA microarray analysis

Isolated total RNA was analyzed by DNA microarray analysis using the human genome U133 set (Affymetrix, Santa Clara, CA, USA), which includes-33,000 human genes, according to the standard protocol recommended by Affymetrix (http://www.affymetrix.com/support/technical/manual/expression manual.affx) [10]. Gene intensity information was converted to a mean intensity for each gene by a proprietary software, Suite ver. 4.0 (Affymetrix), which includes routines for filtering and normalization. The intensity information was then transferred to an Excel software program (Microsoft Japan, Tokyo, Japan) and analyzed as needed.

Gene ontology analysis

A Gene Ontology (GO) database (as of September 18, 2009) was downloaded from the Gene Ontology website (http://www.geneontology.org/). GO analysis was performed with a software package, GeneSpring

ver. 8.0 (Agilent Technologies Santa Clara, CA, USA) [11]. GO analysis identified affected genes and created an "Entity List" on the basis of information gained in the array analysis. GO analysis further calculated the probability of matching between the database and the "Entity List". Probability values less than 0.05 were considered to indicate statistical significance.

Real-time reverse transcription and polymerase chain reaction

To confirm the expression of representative genes, we performed real-time reverse transcription and polymerase chain reaction (RT-PCR) analysis with the appropriate primers (Table 1) and SYBR Green dye using a real-time PCR system (model ABI 7300; Applied Biosystems, Foster City, CA, USA) according to the manufacturer's instructions [12]. Briefly, first-strand cDNAs were reverse transcribed at 42°C for 60 min and 95°C for 5 min from 1 μg of the extracted total RNA with Moloney murine leukemia virus reverse transcriptase (Promega, Madison, WI, USA) and primers (oligo-dT15 primer:random nonamer=1:10). The reaction mixture containing reverse-transcribed cDNAs was preheated for 2 min at 50°C and for 10 min at 95°C to activate *Taq* polymerase. A 40-cycle two-step PCR was performed, consisting of 15 sec at 95°C and 1 min at 60°C. The amount of target mRNA was calculated in the linear phase and normalized using glyceraldehyde-3-phosphate dehydrogenase (GAPDH) as an internal standard according to the delta-delta Ct method [13].

RESULTS

Cross sectional area of semitendinosus muscle in the affected limb

Table 2 shows the CSA of the semitendinosus muscles in the affected limb before and after the exercise period. After the exercise, CSA had increased in size by 4.2 and 14.7%, respectively, in the two hybrid exercise subjects, and by 1.4% in the subject with electrical stimulation. However, it had shrunk by 7.7% in the subject without electrical stimulation. One hybrid exercise subject, a 16-year-old male, started the

TABLE 1.
Primers for the polymerase chain reaction

Target gene	Sequence	Length (bp)
EIF5A	S:5'-CACCCCACAGAGCAAGTTTT-3'	148
	AS:5'-AGCACCACAAAGCCATTCTT-3'	
PEX6	S:5'-CAGAATTCAGAGGTACTTGGAAGG -3'	176
	AS:5'-CCCTGGGTATCTGAAAGTGC-3'	
FHOD3	S:5'-GTCTGAGCTATGCGGAGGAC-3'	170
	AS:5'- ATTGGGCGAGTCATCAGTTC-3'	
GAPDH	S: 5'-ACCCAGAAGACTGTGGATGG-3'	125
	AS: 5'-TTCAGCTCAGGGATGACCTT-3'	

AS, antisense primer; S, sense primer; EIF5A, eukaryotic translation initiation factor 5A; PEX6, peroxisomal biogenesis factor 6; FHOD3, formin homology 2 domain containing 3; GAPDH, glyceraldehyde-3-phosphate dehydrogenase.

TABLE 2.
Profile of subjects and cross-sectional area (CSA) of semitendinosus muscles in the affected limb before and after exercise period

exercise	age gender	after injury (weeks)	CSA of semitendinous muscle		
			before (mm^2)	after (mm^2)	after/before ratio (%)
hybrid	16 yrs old male	24	901	940	104.2
	24 yrs old male	12	633	726	114.7
electrical stimulation	16 yrs old male	16	780	790	101.4
without electrical stimulation	15 yrs old female	8	372	343	92.3

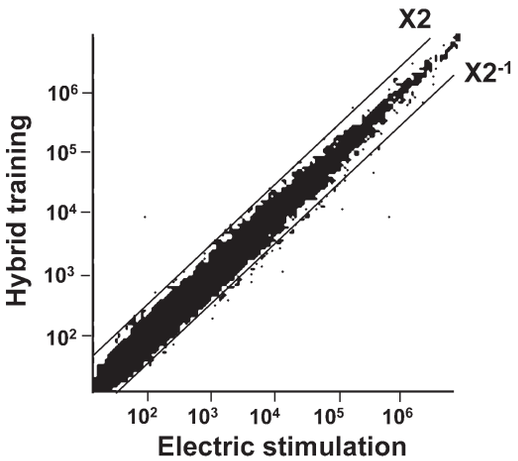

Fig. 3. Gene expression in the semitendinosus muscle.

The gene expression in hybrid exercise was compared with that in electrical stimulation. Genes with a similar expression lie on a line from the origin to the top right corner; the expression level is indicated by the distance from the origin. The scale on each axis is log scale.

exercise 24 weeks after injury. CSA was 901 mm^2 before the exercise and 940 mm^2 after the exercise. The ratio of CSA after/before exercise was 104.2%. The other hybrid exercise subject, a 24-year-old male, started the exercise 12 weeks after injury. CSA was 633 mm^2 before the exercise and 726 mm^2 after the exercise. The ratio of CSA after/before exercise was 114.7%. The subject with electrical stimulation, a 16-year-old male, started the exercise 16 weeks after injury. CSA was 780 mm^2 before the exercise and 790 mm^2 after the exercise. The ratio of CSA after/before exercise was 101.4%. The subject without electrical stimulation, a 15-year-old female, started the exercise 8 weeks after injury. CSA was 372 mm^2 before the exercise and 343 mm^2 after the exercise. The ratio of CSA after/before exercise was 92.3%.

Comprehensive gene expression and GO analyses

The samples were analyzed with a microarray, and a scatter plot was generated (Fig. 3). Genes with an absolute value of less than 500 were excluded. Genes that exhibited increased or decreased levels of expres-

TABLE 3.
Functional classification of 125 genes (Up, top 75 genes; Down, top 50 genes) that exhibited increased or decreased expression levels after hybrid exercise in comparison to electrical stimulation

	Up	Down
Membrane receptor	1	0
Transporter and channel	3	1
Gene expression control		
Signal transduction	14	3
Transcription-related	10	9
Translation-related	2	2
Adhesion and membrane protein	2	2
Cell structure, including cytokinesis, sorting, fusion, and motor protein and motor protein	8	1
Growth factor, secreted protein, and matrix protein and motor protein	1	0
Metabolism	4	4
Mitochondrial protein and gene	2	1
Cell cycle	1	3
Heat shock protein and chaperonin	0	0
Stress response gene	1	0
Heat shock protein and chaperonin	0	0
Ubiquitin-proteasome-related gene	5	4
Other protease-related gene	2	0
Apoptosis	0	1
EST and others	19	19
total	75	50

The sequences of expression sequence tag (EST) genes were subjected to the BLAST retrieval system to search for similar genes.

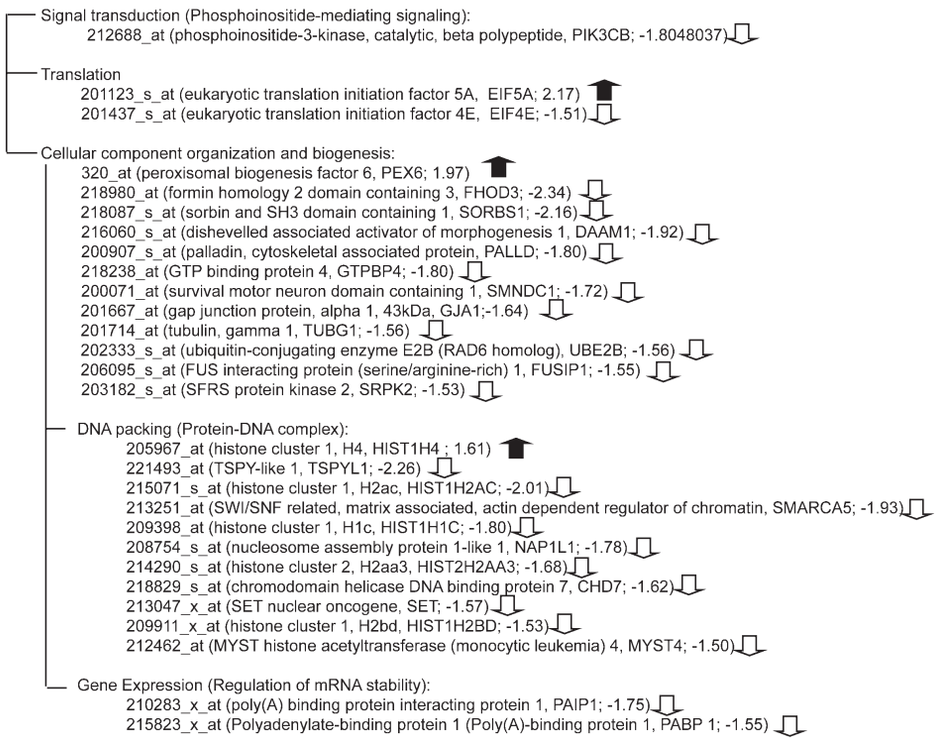

Fig. 4. GO analysis.

GO analysis was performed with a software package, GeneSpring ver. 8.0 (Agilent Technologies). GO analysis classified genes on microarray chips to potent affected genes as "Entity List" on the basis of information gained array analysis. GO analysis further calculates the probability of matching the accurate probability test (direct probability) from the list of categorized "Entity List". Probability values less than 0.05 were considered to be statistically significant.

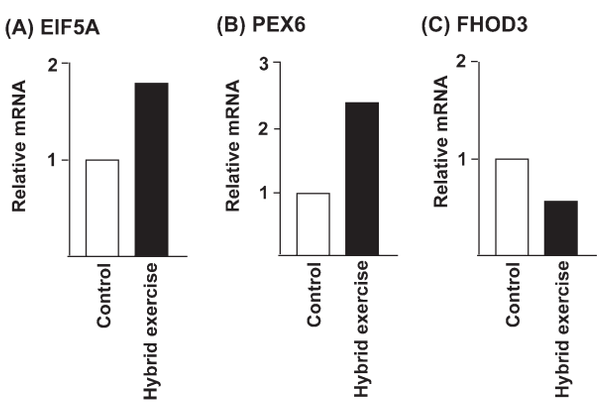

Fig. 5. Expression of EIF5A, PEX6 and FHOD3 in semitendinosus muscles.

Expression of EIF5A (A), PEX6 (B) and FHOD3 (C) transcripts in semitendinosus muscles was assessed by real-time RT-PCR analysis. The fluorescence ratio of the target gene cDNA to GAPDH, a house keeping gene, was calculated. Data are shown as the mean in the hybrid exercise group (n=2), compared with the mean in the control 1 (electrical stimulation, n=1) and control 2 (without electrical stimulation, n=1) groups.

sion were chosen and their functions were classified (Table 3). The results showed that hybrid exercise preferentially promoted the expression of genes associated with signal transduction (14 genes) transcription (10 genes) and cell structure (7 cytoskeletal genes, and 1 sorting gene).

Because the number of candidates for the experiments was limited, we were unable to obtain a sufficient number of skeletal muscles for statistical analysis during this experiment period. Therefore, we performed GO analysis to classify the genes that were significantly changed by hybrid exercise. The GO analysis revealed that hybrid exercise induced significantly higher expression levels of several genes, i.e. eukaryotic translation initiation factor 5A (EIF5A), peroxisomal biogenesis factor 6 (PEX6), and histone cluster 1 H4 (HIST1H4), compared with electrical stimulation alone (Fig. 4). In contrast, the expression of various genes associated with signal transduction, translation, and cellular component organization and biogenesis was suppressed by hybrid exercise (Fig. 4).

We also confirmed the effect of hybrid exercise on the expression of some of these genes by real-time RT-PCR (Fig. 5).

DISCUSSION

"Hybrid exercise" is an exercise method that combines electrically stimulated and volitional contraction. When the joint is volitionally flexed, the extensor muscle is electrically stimulated, and when the joint is volitionally extended, the flexor muscle is electrically stimulated. Therefore, hybrid exercise achieves adequate loading of muscles during both extensor and flexor movements.

In ACL reconstruction surgery, the semitendinosus tendon is prepared as a self-graft. A small amount of muscle attached to this tendon, which was redundant for the graft, was collected during the operation. Hybrid exercise was performed with these preoperative ACL-injured patients, and the muscle tissue which would have been abandoned was used in the experiment. This was why we used ACL-injured patients as the subjects for this study. However we were unable to obtain a sufficient number of skeletal muscles for statistical analysis during the experimental period because the number of candidates was limited.

Preoperative quadriceps strength is considered a significant predictor of knee function after ACL reconstruction surgery [14], and quadriceps exercise has been widely performed before reconstruction surgery. The current study was carried out to evaluate the mechanism of the effect of hybrid exercise and not to show its efficacy in ACL-injured patients. To prove the clinical efficacy of hybrid exercise in ACL-injured patients, a large clinical trial will be required in future.

To elucidate the mechanism of the apparent beneficial effect of hybrid exercise, we examined the comprehensive gene expression profiles in muscles trained by hybrid exercise and compared them with the profiles in control muscles subjected to electrical stimulation alone or without electrical stimulation. The microarray analysis showed that hybrid exercise preferentially promoted the expression of genes associated with signal transduction and transcription, and cytoskeletal genes, as compared with electrical stimulation alone. Our results suggest that hybrid exercise helps to maintain muscle mass after unloading, possibly through this distinct gene expression pattern, although additional studies with larger patient groups will be needed to substantiate this hypothesis.

This is the first report to address the relationship between gene expression and the effect of hybrid exercise. Future GO analyses based on the microarray information obtained herein may further clarify the mechanisms of the beneficial effects of hybrid exercise. The present GO analysis revealed that hybrid exercise induced significantly higher expression of EIF5A and PEX6, compared with electrical stimulation alone, while expression of a variety of genes was suppressed by hybrid exercise. EFA5A is a translation initiation factor, and has previously been shown to have a strong association with the protein synthesis process [15]. Muscle protein synthesis plays a central role in the recovery from muscle atrophy or aging. In fact, the reduction of the EFA5A level in the cerebellum contributes to the impairment of long-term motor memory that is observed during aging [16]. Furthermore, EIA5A enhances muscle regeneration through its role in satellite cell (skeletal muscle stem cell) differentiation [17]. In contrast, peroxisome biogenesis, for which PEX6 is a prerequisite factor [18], plays an important role in muscle regeneration after injury [19].

On the basis of these findings, we suggest that hybrid exercise may stimulate muscle regeneration, perhaps through enhanced expression of EIF5A and PEX6, and may thereby contribute to muscle strengthening. Further studies will be needed to confirm this hypothesis.

ACKNOWLEDGMENTS: We would like to thank Takashi Maeda PT for his valuable assistance in the hybrid exercise. We also thank Yoshio Takano PT for CSA measurement. This study was carried out as part of the "Ground-based Research Announcement for Space Utilization" promoted by the Japan Space Forum.

REFERENCES

1. Matsuse H, Shiba N, Umezu Y, Nago T, Tagawa Y et al. Muscle training by means of combined electrical stimulation and volitional contraction. Aviat Space Environ Med 2006; 77:581-585.
2. Iwasaki T, Shiba N, Matsuse H, Nago T, Umezu Y et al. Improvement in knee extension strength through training by means of combined electrical stimulation and voluntary muscle contraction. Tohoku J Exp Med 2006; 209:33-40.
3. Takano Y, Haneda Y, Maeda T, Sakai Y, Matsuse H et al. Increasing Muscle Strength and Mass of Thigh in Elderly People with the Hybrid-Training Method of Electrical Stimulation and Volitional Contraction. Tohoku J Exp Med 2010; 221:77-85.
4. Yanagi T, Shiba N, Maeda T, Iwasa K, Umezu Y et al. Agonist contractions against electrically stimulated antagonists. Arch Phys Med Rehabil 2003; 84:843-848.
5. Jagoe RT, and Goldberg AL. What do we really know about the ubiquitin-proteasome pathway in muscle atrophy? Curr Opin Clin Nutr Metab Care 2001; 4:183-190.

6. Rommel C, Bodine SC, Clarke BA, Rossman R, Nunez L et al. Mediation of IGF-1-induced skeletal myotube hypertrophy by PI(3)K/Akt/mTOR and PI(3)K/Akt/GSK3 pathways. Nat Cell Biol 2001; 3:1009-1013.
7. Bodine SC, Stitt TN, Gonzalez M, Kline WO, Stover GL et al. Akt/mTOR pathway is a crucial regulator of skeletal muscle hypertrophy and can prevent muscle atrophy in vivo. Nat Cell Biol 2001; 3:1014-1019.
8. Ogino M, Shiba N, Nagata K, Iwasa K, Tagawa Y et al. MRI quantification of muscle activity after volitional exercise and neuromuscular electrical stimulation. Am J Phys Med Rehabil 2002; 81:446-451.
9. Ward AR, and Shkuratova N. Russian electrical stimulation: the early experiments. Phys Ther 2002; 82:1019-1030.
10. Nikawa T, Ishidoh K, Hirasaka K, Ishihara I, Ikemoto M et al. Skeletal muscle gene expression in space-flown rats. FASEB J 2004; 18:522-524.
11. Nelson GM, Ahlborn GJ, Delker DA, Kitchin KT, O'Brien TG et al. Folate deficiency enhances arsenic effects on expression of genes involved in epidermal differentiation in transgenic K6/ODC mouse skin. Toxicology 2007; 241:134-145.
12. Ogawa T, Nikawa T, Furochi H, Kosyoji M, Hirasaka K et al. Osteoactivin upregulates expression of MMP-3 and MMP-9 in fibroblasts infiltrated into denervated skeletal muscle in mice. Am J Physiol Cell Physiol 2005; 289:C697-707.
13. Livak JK, and Schmittgen TD. Analysis of relative gene expression data using real-time quantitative PCR and the 2(-Delta Delta C(T)) Method. Methods 2001; 25:402-408.
14. Eizen I, Holm I, and Rsiberg MA. Preoperative quadriceps strength is a significant predictor of knee function two years after anterior cruciate ligament reconstruction. Br J Sports Med 2009; 43:371-376.
15. Kang HA, and Hershey JW. Effect of initiation factor eIF-5A depletion on protein synthesis and proliferation of Saccharomyces cecervisiae. J Biol Chem 1994; 269:3934-3940.
16. Luchessi AD, Cambiaghi TD, Alves AS, Parreiras-E-Silva LT, Britto LR et al. Insights on eukaryotic translation initiation factor 5A (eIF5A) in the brain and aging. Brain Res 2008; 4:1228:6-13.
17. Luchesi AD, Cambiaghi TD, Hirabara SM, Lambertucci RH, Silveira LR et al. Involvement of eukaryotic translation initiation factor 5A (eIF5A) in skeletal muscle stem cell differentiation. J Cell Physiol 2009; 218:480-489.
18. Fujiki Y, Miyata N, Matsumoto N, and Tamura S. Dynamic and functional assembly of the AAA peroxins, Pex1p and Pex6p, and their membrane receptor Pex26p involved in shuttling of the PTS1 receptor Pex5p in peroxisome biogenesis. Biochem Soc Trans 2008; 36:109-113.
19. Matsuura T, Li Y, Giacobino JP, Fu FH, and Huard J. Skeletal muscle fiber type conversion during the repair of mouse soleus: potential implications for muscle healing after injury. J Orthop Res 2007; 25:1534-1540.

Original Contribution

Kurume Medical Journal, 57, 109-115, 2010

Brain Activities on fMRI Using the *shiritori* Task in Normal Subjects

MASAYUKI INOUE*,**, TAKEFUMI UENO**,†,‡, KIICHIRO MORITA**,
YOSHIHISA SHOJI§, TOSHIMASA MATSUOKA§, RYO FUJIKI§,
TOSHI ABE§§ AND NAOHISA UCHIMURA§

**Kawanonajima Hospital, Fukuoka 813-0043, **Cognitive and Molecular Research Institute of Brain Diseases, Kurume University, Kurume 830-0011, †Department of Neuropsychiatry, Kyushu University Graduate School of Medical Sciences, Fukuoka 812-8582, ‡Department of Rehabilitation, International University of Health and Welfare, Ohkawa 831-8501, Departments of Neuropsychiatry§ and Radiology§§ Kurume University School of Medicine, Kurume 830-0011, Japan*

Received 16 July 2010, accepted 20 October 2010

Edited by TAKAYUKI TANIWAKI

Summary: *Shiritori* is a popular Japanese word chain game that resembles verbal fluency tasks used in Western countries. Recently, *shiritori* has been used to determine the dominant hemisphere for language and as a rehabilitation tool. However, there are few reports of neuroimaging during *shiritori*. We used functional magnetic resonance imaging (fMRI) to conduct a detailed study of brain activities during *shiritori* and observed activation not only of the left inferior frontal gyrus (including the pars opecularis, the pars triangularis and the pars orbitalis), which is a language-related area, but also of the left superior and middle frontal gyri, the right pars orbitalis (inferior frontal gyrus), and the right cerebellar hemisphere. *Shiritori* is a useful tool for psychological study and rehabilitation.

Key words *shiritori*, localization of brain activities, fMRI, word game, frontal gyrus

INTRODUCTION

Different languages produce different types of word games. Japanese word games, for example, often involve palindromes and puns. *Shiritori* is a Japanese word game that enjoys wide popularity among men and women of all ages and occupations (*shiritori* is described later). Recently *shiritori* has attracted attention in Japan as a cognitive rehabilitation tool. However, there are few reports of neuroimaging during *shiritori*. In reported studies, identification of the dominant hemisphere related to language was a major goal but the localization was very rough [1]. Yamamoto et al. [2] performed magnetoencephalography (MEG) in subjects playing *shiritori* and reported left-sided dominance of inferior frontal and superior temporal gyrus activities; however, they did not examine the entire brain including the cerebellum. Moreover, no comparative statistical studies have been performed of brain activities during *shiritori* between males and females.

Detailed examination of *shiritori* may lead to development of more effective rehabilitation techniques in future. In the present study we used high magnetic field MRI during a *shiritori* task to observe activation of brain structures at high resolution, and to enable a

Corresponding author: Masayuki Inoue, Kawanonajima Hospital, Najima 4-28-53, Fukuoka 813-0043, Fukuoka, Japan. Tel: +81-92-681-5231 Fax: +81-92-672-1525 E-mail: inouemas64@gmail.com

Abbreviations: AAL, automated anatomical labeling; ANOVA, analysis of variance; DICOM, digital imaging and communication in medicine; EPI, echo planar imaging; fMRI, functional magnetic resonance imaging; FOV, field of view; MATLAB, matrix laboratory; MEG, magnetoencephalography; PET, positron emission tomography; SPM, statistical parametric mapping; TE, echo time; TR, repetition time

MASAYUKI INOUE and TAKEFUMI UENO equally contributed to this work.

direct comparison of brain activity between males and females.

MATERIALS AND METHODS

Subjects

Twenty healthy subjects (10 males and 10 females with a mean age of 26.0±2.6 years) participated in this study. They had completed at least 12 years of education. Five of them were in university and 15 of them had finished university. Thus, they were considered to have normal intellectual functions. None had a history of neurological or psychological disorders. All were native speakers of Japanese and were judged from the Edinburgh Handedness Inventory to be right-handed [3]. Adequate informed consent was obtained from all subjects. This study was approved by the Ethical Review Board of Kurume University.

Task Design

Shiritori is a word chain game based on the characteristics of the *kana* phonograms used in the Japanese language. There are 46 *kana*, and each *kana* character represents 1 syllable. *Shiritori* is played as follows: first, a player utters a word at random. The next player must say a word that starts with the last syllable of the word uttered by the previous player, and this is repeated serially among the players until one of them uses a word that ends with the *kana* "n" (Fig. 1). This stops the chain because there are no words that begin with the *kana* "n" in Japanese. The players do not know what word the previous player will say until it is uttered, so *shiritori* can be considered a relatively complex and challenging task.

A: Let's do the shiritori.
B: It is good.
A: Then, from me. Ka-ra-su (crow).
B: su-i-ka (watermelon).
A: ka-me-ra (camera).
B: ・・・ra-i-o-n (lion).
I have said words to get "n" at the end.
・・・・It was defeated.

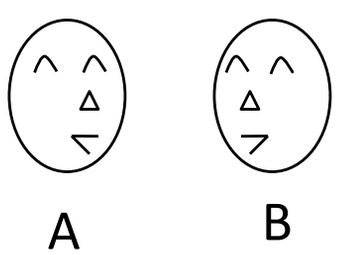

Fig. 1. The method of the *shiritori* task.

In the present study the subjects lay in a supine position with a headset on. The task was composed of 6 blocks of 51 sec each. The subjects were rested in Blocks 1 (Scans 1-10), 3 (Scans 21-30), and 5 (Scans 41-50). They were instructed to keep their eyes open and relax without thinking of anything (rest condition). *Shiritori* was performed in Blocks 2 (Scans 11-20), 4 (Scans 31-40), and 6 (Scans 51-60). The subjects were instructed to keep their eyes open and remain relaxed, as during the rest condition. When the 2nd, 4th, and 6th blocks began, the first word was presented aurally through the headphones. The subjects performed *shiritori* by themselves using the first word without moving their mouth or vocalizing until they were instructed to stop (*shiritori* task condition). The task was orally explained to the subjects at the time of obtaining informed consent. Just before the actual trial the subjects were asked to perform *shiritori* in the waiting room in the presence of a researcher for 50 sec, and the number of words generated was recorded. At this time, *shiritori* was vocalized, unlike during the actual trial.

Data Acquisition

Magnetic resonance imaging was performed on a SIEMENS 1.5 T scanner. T2*-weighted images that covered the whole brain were acquired from each subject using an echo plannar imaging (EPI) pulse sequence echo time (TE) 70 ms, repetition time (TR) 5.1 s, flip angle 90 degrees, field of view (FOV) 225×225×148 mm^3, voxel dimension 64×64×40, slice thickness 3.5 mm). A block paradigm was used in which 10 volumes were controls and 10 volumes were activation periods. One series consisted of 3 periods of activation tasks and 3 periods of rest, yielding a total of 60 volumes of EPI.

Date proproceeing

All the images acquired from the scanner in digital Imaging and communication in Medicine (DICOM) format were converted to Analyze format through the DICOM toolbox in statistical parametric mapping (SPM2) software (Wellcome Department of Cognitive Neurology, London, UK) implemented in matrix laboratory (MATLAB) (Mathworks Inc., Narick, MA) [4]. SPM2 software allowed us to realign all the data to correct for movement. Normalization from each EPI image to the Montreal Neurological Institute EPI reference brain provided by SPM was carried out by resampling to a final size of 2×2×2 mm^3 voxels. Lastly,

smoothing was performed with a Gaussian spatial filter to a final smoothness of 8 mm.

Statistical analysis

Data were analyzed on an individual (subject per subject) basis and across subjects (group analysis) using subject variance (random effect model). For individual analysis, data from each run were modeled using the general linear model with separate functions modeling the hemodynamic response to each experimental epoch. We defined one contrast (*shiritori* task versus rest) for each series (per subject). We first applied a threshold to the T maps at T=7.05 ($p<0.05$, corrected for family-wise error) for the activation task. In these thresholded maps, activated clusters were considered significant if their spatial extent was >8 corresponding to a risk of error (type I error) of $p<0.05$ (corrected). Lastly, activated regions were determined by local maxima labeling of automated anatomical labeling (AAL) [5]. The areas of activated regions were calculated by multiplying the cluster areas determined by SPM by the percentages indicated by cluster labeling of AAL.

In addition, analysis of variance (ANOVA) corrected for sphericity (Greenhouse-Geiser) was applied to the data to determine whether more activated areas existed in one task over another (male > female, or female > male). The F maps were thresholded to F= 10.39 ($p<0.001$) for the main task effect. In these thresholded maps, activated clusters were considered significant if their spatial extent was >54 corresponding to a risk of error (type I error) of $p<0.05$ (corrected).

RESULTS

The average number (±standard deviation) of words that the subjects uttered during the vocal *shiritori* (test trial) before scanning was 24±3.9. After the actual trial the subjects reported that their performances had been about the same as in the test trial in front of the researcher. Figure 2 shows functional magnetic resonance imaging (fMRI) images during the *shiritori* task. In the left hemisphere, the superior frontal gyrus, the middle frontal gyrus, the inferior frontal gyri, the supplementary motor area, the precentral gyrus, the temporal pole: superior temporal gyrus, the insula, the pallidum, the thalamus, and the cingulum were activated during *shiritori* as compared with the rest conditions. In the right hemisphere, the pars orbitalis of the inferior frontal gyrus, insula, and the putamen were activated. Concerning the frontal lobe, while significant activation was observed in an area of 534 voxels on the left side, only 12 voxels were activated on the right side. In the cerebellum, both hemispheres were activated. However, the right hemisphere was activated widely rather than the left hemisphere. Tables 1 and 2 show the activated sites and their areas.

There were no significant differences in the average number (±standard deviation) of words produced in vocal *shiritori* between males and females (males

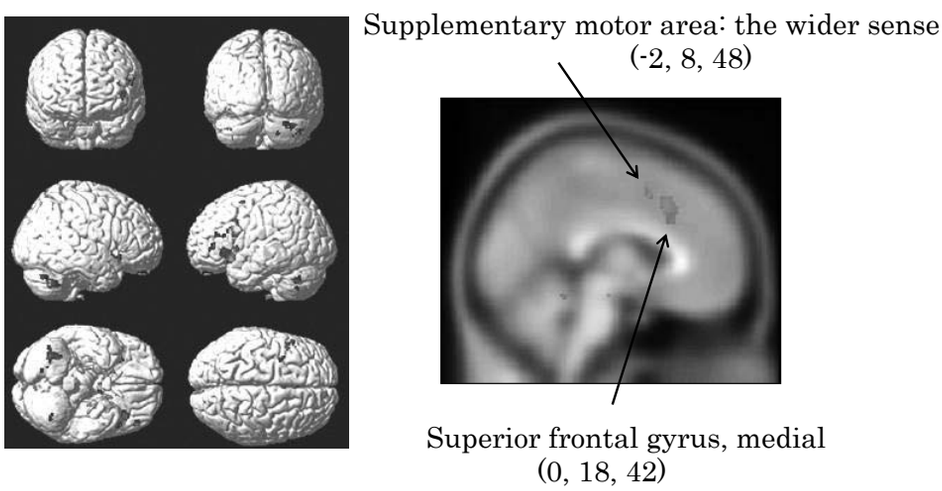

Fig. 2. fMRI images during the *shiritori* task. Significant activation was observed mainly on the left frontal area and the right cerebellum (left). Significant activation was observed in the left medial superior frontal gyrus and the left supplementary motor area: the wider sense. (right) ($p<0.05$, corrected by family-wise error).

TABLE 1.
Locating and p-values

	Region	Coordinate (x, y, z mm)	Voxel-level T-value	Cluster-level (p-value)
left	inferior frontal gyrus pars opercularis	–52, 12, 22	12.69	6.28×10^{-12}
	inferior frontal gyrus pars orbitalis	–36, 26, –4	10.35	3.23×10^{-17}
	Cerebellum Crus1	–38, 60, –36	9.06	1.73×10^{-6}
	inferior frontal gyrus pars trianglaris	–44, 40, 4	8.19	1.84×10^{-4}
	middle frontal gyrus	–32, 4, 56	8.06	0.0054
	inferior frontal gyrus pars trianglaris	–38, 28, 16	8.04	1.15×10^{-5}
	Thalamus	–6, –16, 0	7.91	3.53×10^{-4}
	anterior cingulum	–4, 22, 30	7.87	6.57×10^{-8}
	inferior frontal gyrus pars trianglaris	–48, 24, 22	7.67	0.0160
	supplementary motor area: the wider sense	–2, 8, 48	7.65	1.15×10^{-4}
	Cerebellum 7b	–36, –60, –46	7.41	0.0257
right	Cerebellum 7b	36, –58, –42	11.65	5.07×10^{-21}
	Insula	32, 20, –8	10.56	5.42×10^{-14}
	Cerebellum 8	18, –72, –42	8.45	0.0329

In the same cluster, only the coordinate of highest T-values are shown

TABLE 2.
Volume summary (activated region and percentages per cluster)

	x, y, z mm	Region	%	Number of voxel
left	–52, 12, 22	inferior frontal gyrus pars opercularis	61.5	115
		inferior frontal gyrus pars trianglaris	25.1	47
		precentral gyrus	10.7	20
	–36, 26, –4	Insula	37.43	125
		inferior frontal gyrus pars orbitalis	33.53	112
		inferior frontal gyrus pars trianglaris	10.48	35
		temproral pole: superior temporal gyrus	7.78	26
		inferior frontal gyrus pars opercularis	5.69	19
	–16, –2, –10	Pallidum	9.24	11
	–38, –60, –36	Cerebellum Crus1	88.41	46
	–44, 40, 4	inferior frontal gyrus pars trianglaris	91.67	33
	–32, 4, 56	middle frontal gyrus	94.12	16
	–38, 28, 16	inferior frontal gyrus pars trianglaris	71.79	28
		middle frontal gyrus	23.08	9
	–6, –16, 0	Thalamus	96.88	31
	–4, 22, 30	middle cingulum	35.42	34
		superior frontal gyrus, medial	33.33	32
		supplementary motor area: the wider sense	18.75	18
		anterior cingulum	10.42	10
	–48, 24, 22	inferior frontal gyrus pars trianglaris	100	12
	–2, 8, 48	supplementary motor area: the wider sense	97.44	38
right	36, –58, –42	Cerebellum Crus1	54.17	247
		Cerebellum 6	21.49	98
		Cerebellum 8	6.36	29
		Cerebellum Crus2	3.51	16
		Cerebellum 7b	1.97	9
	32, 20, –8	Insula	60.17	145
		Putamen	6.64	16
		inferior frontal gyrus pars orbitalis	4.98	12
	18, –72, –42	Cerebellum 8	100	9

23.4±4.1, females 24.2±3.9, P=0.66: unpaired t-test, P=0.63: Mann-Whitney U test), and there were no significant differences between males and females in the brain activation patterns by fMRI (one-way ANOVA, $P<0.001$).

DISCUSSION

In the healthy subjects, activation of the left side of the cerebrum was predominant during *shiritori*.

Concerning the frontal lobe, while significant activation was observed in an area of 534 voxels on the left side, only 12 voxels were activated on the right side, and activities of the frontal lobe were also markedly left-sided. The medial superior frontal gyrus has been suggested to have a central role in encoding response conflict [6]. We considered that response conflict might occur during *shiritori* in the process of searching for an appropriate word while excluding inappropriate words (words that end with the *kana* "n"). Our results appear to have confirmed this hypothesis.

The middle frontal gyrus has been reported to show significant left-sided dominance in many language-related tasks, and this is considered to be due to the process of word generation [7] and the use of working memory [8]. Narayanan et al. [9] divided the process of working memory into smaller units using a verbal fluency task and showed the activation of this site in encoding, maintenance, and retrieval phases. Since *shiritori* basically involves the same psychological processes as the verbal fluency task, the activation of the left middle frontal gyrus observed in our study appears reasonable. Concerning the inferior frontal gyrus, the pars triangularis and pars opercularis comprise Broca's area and are related to linguistic processing and the production and understanding of vocal and sign languages [10]. This area is widely known to be related to speech, as demonstrated by the occurrence of motor aphasia following its impairment. Since it has been shown to be activated by silent verbal tasks similar to those used in this study [2,11], it is considered to be involved in word recall and retrieval processes. As to the function of pars orbitalis, it has been implicated in the semantic processing of language [12-14]. Furthermore, although it is thought to be related to inhibitory control [15,16] and motivation [17, 18], these are usually associated with activation of both sides. Our study showed that the pars orbitalis was activated bilaterally. In *shiritori* it is against the rules to say a word ending in "n". When subjects noticed that they were about to use an inappropriate word, it is possible that inhibitory control acted and the pars orbitalis was activated bilaterally. Moreover, in our study, the subjects received no reward. However, when interviewed after the end of the experiment, all subjects showed interest in their performances, so this area is considered to have been activated due to a motivation to perform well.

The precentral gyrus, a primary motor area, was activated particularly below the center, the area controlling the lips, in this study. The subjects were instructed not to move their lips, and their compliance regarding this instruction was confirmed after the experiment. Similar activation of the precentral gyrus was reported in previous studies [2,8,11], which suggested the possibility of its activation by imaging of vocalization and slight lip movements, despite instruction to avoid them. In this study, activation of the supplementary motor area was also indicated by AAL. In the AAL that we used, the pre-supplementary motor area and the supplementary motor area (proper) were not classified separately, and the whole region was treated as the supplementary motor area in the wider sense [5]. In this study the anterior part of the supplementary motor area was activated during *shiritori*, so we regarded this part as the pre-supplementary motor area. It is reported that the pre-supplementary motor area is associated with conscious response inhibition [19]. We considered that this region was activated by conscious response inhibition to avoid using inappropriate words.

Concerning the cerebellum, many areas of the right cerebellar hemisphere were activated, but only the crus1 was activated in the left hemisphere, showing clear right-sided dominance. Relationships of the cerebellum with various higher cognitive functions have been reported. Regarding linguistic functions, Peterson et al. [20] reported activation of the right cerebellar hemisphere using positron emission tomography (PET) during the task of thinking of appropriate verbs for acoustically or visually presented nouns. Therefore, they considered that this activation was related to cognitive activities of the brain rather than to the mere repetition of words or motor functions. Activation of the cerebellum in our study is also considered to have been due to cognitive linguistic activities. Activation of the cerebellum has also been reported with activation of the frontal lobe [20,21]. In addition, Peterson et al. [20] noted activation of the left frontal lobe and right cerebral hemisphere, and suggested functional as well as anatomical cross-communication between the frontal lobe and cerebellum. Furthermore, Hubrich-Ungureanu et al. [22] indicated that cerebellar activation was contralateral to the activation of the frontal cortex using fMRI during a verbal fluency task. Our results confirm the contralateral cerebellar activation.

In addition, we looked for differences between the male and female groups, but there were no significant differences in the executed number of *shiritori* or in the regions activated during this task. Bell et al. [23], however, reported that males had a significantly greater mean activation than females in a covered word generation task. In explaining the identified gender difference, they reasoned that females would be expected to perform better on verbal tasks than males although they did not have performance data on this owing the nature of the task. In our *shiritori* task, the practice results before the scan revealed no significant difference in performance of word generation between males and females. Furthermore, the subject interviews performed after fMRI indicated that the number of *shiritori* words was the same for males and females. In contrast to Bell's result, performance in the present study was the same in both groups. This may be why fMRI activation was the same in the female and male groups.

In this study of healthy Japanese subjects, the *shiritori* task clearly showed left cerebral hemisphere predominance, and the utility of this task for identification of the predominant hemisphere in language use was confirmed. High magnetic field MRI showed that the *shiritori* task bilaterally activated the pars orbitalis, which is seldom activated by conventional verbal fluency tasks, indicating that the subjects might be more easily motivated to perform *shiritori* than other language tasks. Moreover, it has been shown that *shiritori* involved the interaction of various areas of the brain. In future, we plan to take advantage of the characteristics of the *shiritori* task in the treatment of psychiatric patients, such as those with schizophrenia. Our findings suggest that *shiritori* may be a useful tool for psychological study and rehabilitation.

ACKNOWLEDGMENTS: This work was supported by a Grant-in-Aid for Scientific Research KAKENHI (No. 20790846) from MEXT. The authors thank Daniel Mrozek for correcting grammatical errors.

REFERENCES

1. Takayama H, Kobayashi M, Sugishita M, Onozuka S, and Kawase T. Determination of language lateralization using functional MRI during performance of SHIRITORI tasks in neurosurgery patients. Jpn J Neurosurg 2001; 10:155-163. (in Japanese)
2. Yamamoto M, Ukai S, Shinosaki K, Ishii R, Kawaguchi S et al. Spatially filtered magnetoencephalographic analysis of cortical oscillatory changes in basic brain rhythms during the Japanese 'Shiritori' Word Generation Task. Neuropsychology 2006; 53:215-222.
3. Oldfield RC. The assessment and analysis of handedness: the Edinburgh inventory. Neuropsychologia 1971; 9:97-113.
4. Friston KJ, Holmes AP, Poline J-B, Grasby PJ, Williams SC et al. Analysis of fMRI Time-Series Revised. Neuroimage 1995; 2:45-53.
5. Tzourio-Mazoyer N, Landeau B, Papathanassiou D, Crivello F, Etard O et al. Automated anatomical labeling of activations in SPM using a macroscopic anatomical parcellation of the MNI MRI single-subject brain. Neuroimage 2002; 15:273-289.
6. Rushworth MF, Walton ME, Kennerley SW, and Bannerman DM. Action sets and decisions in the medial frontal cortex. Trends Cogn Sci 2004; 8:410-417.
7. Frith CD, Fristone KJ, Liddle PF, and Frackowiak RS. A PET study of word finding. Neuropsychologia 1991; 29:1137-1148.
8. Cuenod CA, Bookheimer SY, Hertz-Pannier L, Zeffiro TA, Theodore WH et al. Functional MRI during word generation, using conventional equipment: a potential tool for language localization in the clinical environment. Neurology 1995; 45:1821-1827.
9. Narayanan NS, Prabhakaran V, Bunge SA, Christoff K, Fine EM et al. The role of the prefrontal cortex in the maintenance of verbal working memory: an event-related FMRI analysis. Neuropsychology 2005; 19:223-232.
10. Horwitz B, Amunts K Bhattacharyya R, Patkin D, Jeffries K et al. Activation of Broca's area during the production of spoken and signed language: a combined cytoarchitectonic mapping and PET analysis. Neuropsychologia 2003; 41:1868-1876.
11. Rueckert L, Appollonio I, Grafman J, Jezzard P, Johnson R Jr et al. Magnetic resonance imaging functional activation of left frontal cortex during covert word production. J Neuroimaging 1994; 4:67-70.
12. Costafreda SG, Fu CHY, Lee L, Everitt B, Brammer MJ et al. A Systematic Review and Quantitaive Appraisal of fMRI Studies of Verbal Fluency: Role of the Left Inferior Frontal Gyrus. Hum Brain Mapp 2006; 27:799-810.
13. Badre D, and Wagner AD. Left ventrolateral prefrontal cortex and the cognitive control of memory. Neuropsychologia 2007; 45:2883-2901.
14. Sabb FW, Bilder RM, Chou M, and Bookheimer SY. Working memory effects on semantic processing: priming differences in pars orbitalis. Neuroimage 2007; 37:311-322.
15. de Zubicaray G, McMahon K, Eastburn M, and Pringle A. Top-down influences on lexical selection during spoken word production: A 4T fMRI investigation of refractory effects in picture naming. Hum Brain Mapp 2006; 27:864-873.
16. Schulz KP, Clerkin SM, Halperin JM, Newcorn JH, Tang CY et al. Dissociable neural effects of stimulus valence and preceding context during the inhibition of responses to emotional faces. Hum Brain Mapp 2009; 30:2821-2833.
17. Dolan RJ. The human amygdale and orbital prefrontal cortex in behavioural regulation. Philos Trans R Soc Lond B Biol Sci 2007; 362:787-799.
18. Watanabe M, and Sakagami M. Integration of cognitive and motivational context information in the primate prefrontal cortex. Cereb Cortex 2007; 17:101-109.
19. van Gaal S, Ridderinkhof KR, Scholte HS, and Lamme

VA. Unconscious activation of the prefrontal no-go network. J Neurosci 2010; 30:4143-4150.
20. Peterson SE, Fox PT, Posner MI, Mintun M, and Raichle ME. Positron emission tomographic studies of the processing of single words. J Cogn Neurosci 1989; 1:153-170.
21. Grasby PM, Frith CD, Friston KJ, Simpson J, Fletcher PC et al. A graded task approach to the functional mapping of brain areas implicated in auditory-verbal memory. Brain 1994; 117:1271-1282.
22. Hubrich-Ungureanu P, Kaemmerer N, Henn FA, and Braus DF. Lateralized organization of the cerebellum in a silent verbal fluency task: a functional magnetic resonance imaging study in healthy volunteers. Neurosci Lett 2002; 319:91-94.
23. Bell EC, Willson MC, Wilman AH, Dave S, and Silverstone PH. Males and females differ in brain activation during cognitive tasks. Neuroimage 2006; 30:529-538.

Original Contribution

Kurume Medical Journal, 57, 117-124, 2010

The Prevention of Hip Fracture with Menatetrenone and Risedronate Plus Calcium Supplementation in Elderly Patients with Alzheimer Disease: A Randomized Controlled Trial

YOSHIHIRO SATO, YOSHIAKI HONDA, KAZUO UMENO*, NORIMASA HAYASHIDA*, JUN IWAMOTO**, TSUYOSHI TAKEDA** AND HIDEO MATSUMOTO**

Departments of Neurology and Neuropsychiatry, Mitate Hospital, Tagawa 826-0041 and*
***Institute for Integrated Sports Medicine, Keio University School of Medicine,*
Tokyo 160-8582, Japan

Received 31 May 2010, accepted 25 October 2010

Summary: A high incidence of fractures, particularly of the hip, represents an important problem in patients with Alzheimer disease (AD), who are prone to falls and have osteoporosis. We previously found that vitamin K deficiency and low 25-hydroxyvitamin D (25-OHD) with compensatory hyperparathyroidism cause reduced bone mineral density (BMD) in female patients with AD. This may modifiable by intervention with menatetrenone (vitamin K2) and risedronate sodium; we address the possibility that treatment with menatetrenone, risedronate and calcium may reduce the incidence of nonvertebral fractures in elderly patients with AD. A total of 231 elderly patients with AD were randomly assigned to daily treatment with 45 mg of menatetrenone or a placebo combined with once weekly risedronate sodium, and followed up for 12 months. At baseline, patients of both groups showed high undercarboxylated osteocalcin (ucOC) and low 25-OHD insufficiency with compensatory hyperparathyroidism. During the study period, BMD in the treatment group increased by 5.7% and increased by 2.1% in the control group. Nonvertebral fractures occurred in 15 patients (10 hip fractures) in the control group and 5 patients (2 hip fractures) in the treatment group. The relative risk in the treatment group compared with the control group was 0.31 (95% confidence interval, 0.12-0.81). Elderly AD patients with hypovitaminosis K and D are at increased risk for hip fracture. The study medications were well tolerated with relatively few adverse events and effective in reducing the risk of a fracture in elderly patients with AD.

Key words Alzheimer disease, fall, hip fracture, vitamin K deficiency, osteoporosis

INTRODUCTION

Alzheimer disease (AD) is a common neurodegenerative disorder characterized by progressive loss of memory and cognitive function, and far advanced AD is associated with generalized weakness. A high incidence of fractures, particularly of the hip [1-3], represents an important problem in patients with AD, who are prone to falls [4] and may have osteoporosis. The odds ratio reported for fracture prevalence between elderly persons with and without AD is 6.9 [4]. Hip fractures are associated with higher medical costs compared with all other osteoporosis-related fractures combined [5]. Functional recovery after hip fracture in AD is poor [6-8] and patients with dementia have increased mortality during the first 6 months after a hip fracture [9]. The physical condition of patients with AD has increasingly become one of the critical

Corresponding author: Dr. Yoshihiro Sato, Department of Neurology, Mitate Hospital, 3237 Yugeta, Tagawa 826-0041, Japan. Tel: +81-947-44-0924 Fax: +81-947-46-3090 E-mail: y-sato@ktarn.or.jp

Abbreviations: AD, Alzheimer disease; ARR, absolute risk reduction; BI, Barthel index; BMD, bone mineral density; BMI, body mass index; CXD, computed x-ray densitometry; DCC, day care centers; D-Pyr, deoxypyridinoline; FFQ, food frequency questionnaire; MMSE, Mini-Mental State Examination; NNT, number needed to treat; PTH, parathyroid hormone; RR, relative risk; 25-OHD, 25-hydroxyvitamin D; ucOC, undercarboxylated osteocalcin.

issues in their management. We previously demonstrated that deficiency of 25-hydroxyvitamin D (25-OHD) due to sunlight deprivation and vitamin K deficiency due to malnutrition contributed to reduced bone mineral density (BMD) in patients with AD and were associated with a high risk of hip fracture [10,11].

Our previous study demonstrated that menatetrenone (vitamin K2) reduced the risk of hip fracture in patients with AD [11]. We also showed that risedronate and vitamin D plus calcium supplementation prevented the hip fracture in patients with AD [12].

These studies demonstrated low vitamin K and vitamin D deficiency with compensatory hyperparathyroidism contribute to reduced BMD in patients with AD. Nutritional vitamin K1 deficiency [13] may reduce carboxylation of osteocalcin, which may cause reduced BMD in elderly patients with AD [14]. Low dietary vitamin K1 intake was associated with low BMD in women leading to an increased risk of hip fracture [15], and treatment with menatetrenone increases metacarpal BMD in senile osteoporosis [16] and reduces the incidence of fractures in patients with postmenopausal osteoporosis [17]. Menatetrenone therapy would be beneficial for increasing BMD in patients with AD. Risedronate sodium, a pyridinyl bisphosphonate, is known to reduce bone resorption through the inhibition of osteoclastic activity [18]. Risedronate decreases the risk of fractures and increases BMD in postmenopausal women with osteoporosis [19]. According to a recent review [20], the effectiveness of risedronate in preventing osteoporotic fractures has been clearly demonstrated in many trials.

We therefore conducted a 12-month randomized, double-blind trial to evaluate the efficacy of menatetrenone and risedronate for preventing the progression of osteoporosis and decreasing the risk of a nonvertebral fractures in elderly patients with AD. Also, biochemical indexes of bone metabolism were measured to assess the effectiveness of the therapy. Although reduced vitamin D is one of the cause of hip fracture in AD [21], we did not administer vitamin D in the present study because the purpose of the study is to determine effectiveness of menatetrenone, risedronate and calcium without vitamin D supplementation in reducing hip fracture in AD. The Institutional Review Board approved the study with reservation that required us the usage of an external hip protector on patients with the baseline serum 25-OHD level of below 10 ng/mL. The rate of nonvertebral fractures was not determined in this study because many vertebral fractures are asymptomatic in elderly patients with AD and the interpretation of spinal X-ray films may be the presence of osteoarthritis or scoliosis.

METHODS

Study population

This study compared the incidence of vertebral fractures in 2 groups of elderly patients with AD of both genders who were administered menatetrenone or a placebo, combined with risedronate and calcium. The menatetrenone and placebo capsules in this trial were identical in size, weight, color and taste. We recruited 231 ambulatory patients from consecutive patients in our outpatient clinic who were 70 years or older, living in the community and cared for by their family caregivers, and who met criteria for dementia and probable AD according to the Diagnostic and Statistical Manual of Mental Disorders, Revised Third Edition [22]. Patients were recruited from August 2007 to July 2008, and each patient was followed up for 12 months. Patients younger than 70 years were excluded from the study. Patients with impairment of hepatic, renal, cardiac, or thyroid function or those who had known causes of osteoporosis, such as primary hyperparathyroidism, renal osteodystrophy, or familial osteoporosis, were excluded from this study. Also, patients were excluded if they had received any drug known to alter bone metabolism, such as corticosteroids, anticonvulsants, estrogens, calcitonin, bisphosphonate, calcium, or vitamins D and K (all forms), for 3 months or longer during the 12 months preceding the study. The study neurologist (Y.S.), who remained blind to the results of biochemical assays of bone metabolism, diagnosed AD.

Baseline demographic data and duration of illness were obtained. At baseline, we determined body mass index (BMI), and the Mini-Mental State Examination (MMSE) [23] was given to the patients. Activities of daily living were assessed by the Barthel index (BI), in which a functional dependence score of 100 represents independence [24]. Mean weekly intake of dietary vitamin K1 (phylloquinone) during the previous 12 months was calculated for each individual from a questionnaire filled by patients or family members. Daily dietary intake of phylloquinone was assessed by a 126-item semiquantitative food frequency questionnaire (FFQ) [25,26]. Patients who fell at least once in the 3 months before recruitment were defined as "fallers". We assessed the degree sunlight deprivation according to the method of Komar et al. [27]; i.e. sunlight exposure was assessed by the family members and graded as almost none, less than 15 min per week, or 15 min or longer per week. The sunlight exposure

during the preceding year was assessed by the family members when patients spent a time in homes, whereas it was assessed by staff of day care centers (DCC) during patients stay in DCC. This study was approved by the ethics committee of the Mitate Hospital. All patients and controls were informed of the nature of the study. Written informed consent was obtained from each participant or from family members when patients were unable to understand because of dementia.

Study protocol

The patients were assigned to 1 of the 2 study groups by means of computer-generated random numbering. Random allocation sequence was implemented using numbered containers, and the sequence was concealed until interventions were assigned. The patients and all study personnel were blinded to treatment assignment and biochemical measurements. The randomization code was generated using a permuted block size of 4 (stratified by site) by a consulting statistician not otherwise involved in the trial. No other restrictions were used in the randomization procedure. Physicians who performed the follow-up assessment of the patients' condition were blinded to randomization and study group. Patients in the treatment group (n=116) received a daily dose of 45 mg menatetrenone/day in capsule (Glakay, Eizai Pharmaceuticals, Tokyo, Japan) 3 times a day after meals and risedronate (Actonel, Eizai Pharmaceuticals, Tokyo Japan) 17.5 mg once weekly in a tablet and 1200 mg of elemental calcium. The control group received a daily dose of risedronate 17.5 mg once weekly and 1200 mg of elemental calcium (n=115). Patients were instructed to take the tablet with a cup of water (180 mL), 30 to 60 minutes before breakfast, and to remain sitting or maintain an upright position for 60 minutes thereafter. Adherence to study medication was assessed by counting the returned tablets. No dose adjustments were made at any time during the study. Patients were prohibited from taking any other drugs that could affect bone metabolism during the study period.

Follow-up

Assessment of the patients' condition was performed by physicians (Y.S. and Y.H.) who did not participate in the initial randomization.

Both groups were observed for 12 months. General medical evaluation and laboratory values were assessed on entry and after 12 months. The patients' clinical status was assessed at baseline, and all patients were followed up every 4 weeks in the outpatient clinic, at which times nonvertebral fractures were recorded.

Symptomatic nonvertebral fractures confirmed by radiological examinations were considered adverse clinical events, with no attempt to exclude fractures related primarily to trauma. Falls were registered by means of monthly "fall calendars." The family members of participants were instructed to complete the calendar daily, marking an "×" for each fall on the date when the fall occurred. In addition, the characteristics of each fall were recorded according to the timing, direction, and severity of the fall, and the activity in which the fall occurred and injuries due to the fall were also recorded. Both groups were observed for 12 months. General medical evaluation and laboratory values were assessed on entry and 12 months later. Metacarpal BMD measurement was assessed on entry and after 6 and 12 months. Computed x-ray densitometry (CXD, Teijin Diagnostics, Tokyo, Japan) [28] utilizing an improved microdensitometric method was used to quantify BMD in the left second metacarpal of each patient as described previously [10]. The computer algorithm for CXD compares bone radiodensity with the gradations of an aluminum step wedge, calculating bone thickness as an aluminum equivalent (mm Al) showing the same x-ray absorption. The validity and accuracy of this method have been described elsewhere [29]. In the morning, blood and urine samples were obtained from the 231 patients after an overnight fast at study entry and 12 months later. Blood samples were analyzed for ionized calcium, intact parathyroid hormone (PTH), 25-OHD and undercarboxylated osteocalcin (ucOC; a sensitive marker of vitamin K status [30,31]). The cut off value of ucOC in Japanese people is 4.5 ng/mL [32]. Ionized calcium concentration was determined in fresh serum processed under anaerobic conditions using an ion-selective electrode and an ionized calcium analyzer (Jokoh Co., Tokyo, Japan). Serum PTH concentration was measured by an immunoradiometric assay (Sumitomo Biomedical, Osaka, Japan). Ionized calcium was measured in freshly prepared serum collected under anaerobic conditions. An ion-selective electrode was used as part of an ionized calcium analysis system (NOVA Biochemical, Newton, MA, USA). Serum 25-OHD concentration was determined by a radioimmunoassay (DiaSorin, Stillwater, Mich, USA). An electro-chemiluminescence immunoassay was used to measure ucOC in serum samples (Sanko-Biochemicals, Tokyo, Japan). Urinary deoxypyridinoline (D-Pyr) was measured with a commercially available, specific enzyme immunoassay kit (Metra Biosystems Inc, Calif, USA). Urinary D-Pyr was expressed relative to urinary creatinine

concentration. These analyses were carried out in the Central Hormone Reference Laboratory in Kita-kyusyu. The normal ranges of the BMD and biochemical indexes in elderly persons are given in Table 2 [11].

Study end points and statistical analysis

The primary end point was defined as the incidence of a hip fracture. An intention-to-treat analysis was performed on all randomized subjects to determine relative risk (RR), absolute risk reduction (ARR) and the number needed to treat (NNT). The within-group changes from the baseline values were assessed by the paired t test. Group differences of the categorical data were tested by the Fisher exact test. Spearman rank correlation coefficients were calculated to determine the relationships between BMD and serum ucOC, 25-OHD or intact PTH. Laboratory values and BMD were expressed as percentage change from the baseline, and the 2 groups were compared by the Wilcoxon rank sum test. $P<.05$ was considered statistically significant.

The sample size was based on an expected nonvertebral fracture incidence of 10% in the control group over 12 months. Assuming a 10% dropout rate over 12 months, the study had at least 80% power to detect a 70% reduction in fracture risk, with a 2-sided significance level of $\alpha = .05$.

RESULTS

Baseline characteristics of study subjects (Table 1)

Of 263 assessed subjects, 231 were randomized into the treatment groups (Fig. 1). Twenty-three patients in the treatment group and 27 in the control group dropped out or withdrew from the study owing to noncompliance, loss to follow-up, intercurrent illness, or death. Thus, a total of 180 patients (92 in the treatment group

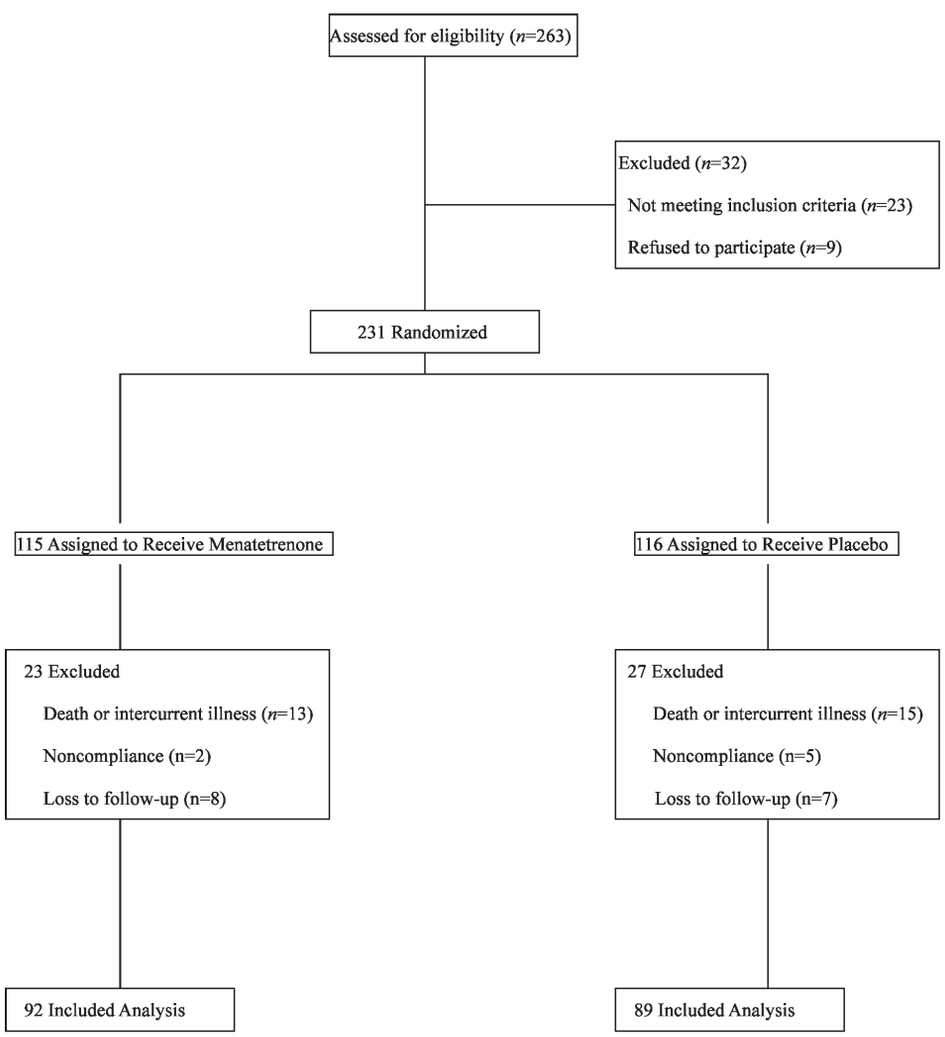

Fig. 1. Flow of participants through the study.

TABLE 1.
Demographic and baseline clinical characteristics of the patients with Alzheimer's disease at study entry

Characteristic	Control group (n=115)	Treated group (n=116)	p value*
Age (years)	80.6±7.4	80.8±7.2	.91
Sex (Men/Women)	38/77	40/76	.82 §
Duration of illness (years)	5.2±2.3	5.1±2.1	.84
Body mass index (kg/m^2)	19.0±2.7 ‖	19.1±2.5 ‖	.92
Mini-Mental State Examination†	17±4 ‖	17±5 ‖	.95
Barthel index	83±5	85±4	.73
Dietary intake of vitamin K1 (μg/day)	98±18 ‖	95±19 ‖	.81
Sunlight exposure/week			
>15 min	25 (22%)	28 (24%)	
<15 min	90 (78%)	88 (76%)	.66§
Faller (%)	36 (31%)	38 (33%)	.87§

Values are mean±SD. *unpaired *t* test; †The mean standard deviation of Mini-Mental Examination scores in cognitively normal subject (mean age 80.3 years, 70% women) has been reported as 28.5±1.4. ; §chi-squared analysis between treated and control groups. Normal Japanese dietary intake of vitamin K1 is 247±102 (μg/day).[11]

TABLE 2.
Bone mineral density and various biochemical tests of control subjects and two groups of patients with Alzheimer's disease at baseline

	Control group	Treated group	P value*
Ionized calcium (mEq/L)	2.42±0.11	2.42±0.12	.92
Intact PTH (pg/mL)	71±14	69±15	.98
25-OHD (ng/mL)	12.6±2.5	12.8±2.8	.90
Deoxypyridinoline (μmol/mol creatinine)	10.0±4.0	10.5±3.7	.87
ucOC (ng/mL)	8.7±2.9	8.9±2.4	.84
Bone mineral density (mm Al)	1.74±0.49	1.74±0.42	.94

Values are mean±SD. * unpaired *t* test; PTH, parathyroid hormone; 25-OHD, 25-hydroxyvitamin D; ucOC, undercarboxylated osteocalcin.
The reference range [11]: ionized calcium, 2.45 to 2.63 mEq/L (ion-selective electrode); intact PTH, 35-63 pg/mL (immunoradiometric assay); 25-OHD, 18.5 to 30.5 ng/mL (competitive protein-binding assay); Deoxypyridinoline, 4.0 to 8.2 μmol/mol creatinin (enzyme immunoassay); bone mineral density, 1.89 to 2.37 mm Al (computed X-ray densitometer).

and 89 in the control group) completed the trial. We included 231 patients in each treatment group in the final intention-to-treat analysis.

Table 1 lists the baseline characteristics of the participants. There was no significant difference between the 2 groups in age, sex, duration of illness, BMI, MMSE, numbers of fallers, BI, sunlight exposure and dietary intake of vitamin K1. BMI was low in both groups. Many of the patients in both groups had been exposed to sunlight for less than 15 min per week or had almost no sun exposure because of being homebound. The average values of dietary intake of vitamin K1 in the 2 groups were lower compared with the previous reported data [11]. As shown in Table 2, in the 2 groups, the baseline values of serum ionized calcium, 25-OHD concentrations were low, whereas serum PTH and ucOC or urinary D-Pyr were high compared with the reference range of the normal Japanese population [11]. Metacarpal BMD in the two patients groups was significantly lower compared with reference range of the normal Japanese population [11]. When both patient groups were analyzed together, the BMD correlated positively with BMI ($r=0.392$; $P<.01$), and 25-OHD ($r=0.428$; $P<.01$) concentrations, whereas BMD correlated negatively with ucOC ($r=-0.701$; $P<.0001$) and PTH ($r=-0.303$; $P<.01$).

There were negative correlations between serum 25-OHD and PTH ($r=-0.213$; $P<.01$), suggesting the presence of compensatory hyperparathyroidism.

Fracture incidence

Hip fractures: There were 2 hip fractures in the treatment group and 10 hip fractures in the control group; this difference was statistically significant ($P<.001$, log-rank test). The number of the hip fractures per 1000 patient-years was 17 and 86 for the treatment and control groups, respectively. The RR, ARR and the NNT in the treatment group as compared with the control group for hip fractures were 0.19 (95% CI, 0.04 to 0.85), 0.09 (95% CI, 0.02 to 0.17) and 11 (95% CI, 6 to 52), respectively.

All fractures: There were 5 fractures in the treatment group and 15 fractures in the control group; this difference was statistically significant ($P<.001$, log-rank test). The unadjusted RR, ARR and NNT in the treatment group as compared with the control group for all fractures were 0.31 (95% CI, 0.12 to 0.81), 0.12 (95% CI, 0.03 to 0.21) and 8 (95% CI, 5 to 36), respectively.

There was no significant difference between the two groups in the number of falls per subject during the 12 months (2.2±1.8 in the control group and 2.3±1.9 in the treated group).

Bone changes and blood biochemical markers

Figure 2 shows the percentage changes from the baseline in metacarpal BMD during the 12 months. The mean ± SD percentage changes in BMD were +5.7±0.8 in the treatment group and +2.2±0.5 in the control group. The difference between the 2 groups was statistically significant ($P<.001$). Changes in various parameters during the 1-year study period are summarized in Table 3. UcOC levels decreased significantly in the treatment group but not in the control group. Urinary levels of D-Pyr decreased while ion-

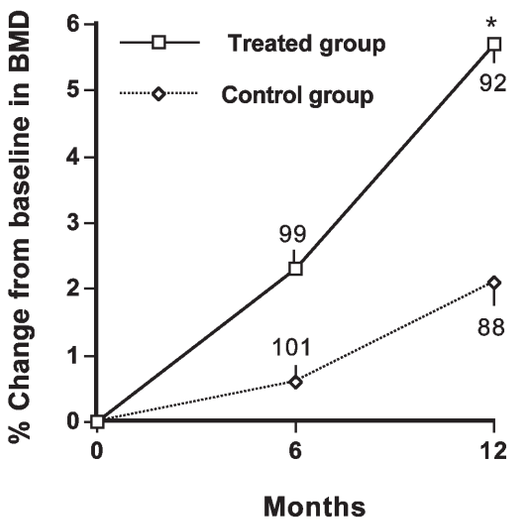

Fig. 2. Percent changes (mean±SE) from baseline in metacarpal bone mineral density (BMD) after 6 and 12 months in the two groups of patients. During the 12 months, the differences in the percent changes in the BMD among the two groups were statistically significant (based on Wilcoxon rank sum test; $p<.001$*). Numbers in parentheses are the numbers of the subjects follow.

TABLE 3.
Selected changes after 1 year in the 192 subjects who completed the study

	Percent change after 1 year (values at 1 year)	*p* value*
Ionized calcium (mEq/L)		
Untreated group	+5.8±0.9 (2.43±0.79)	
Treated group	+5.9±0.4 (2.43±0.86)	.94
Intact PTH (pg/mL)		
Untreated group	-1.3±1.7 (70±11)	
Treated group	+3.2±2.3 (71±10)	.38
25-OHD (ng/mL)		
Untreated group	-5.6±3.8 (11.9±2.9)	
Treated group	-7.1±4.2 (11.7±2.6)	.68
Deoxypyridinoline (μmol/mol creatinine)		
Untreated group	-57.0±13.8 (5.7±1.8)	
Treated group	-46.7±15.5 (5.6±1.9)	.55
ucOC (ng/mL)		
Untreated group	+2.3±1.4 (8.9±2.2)	
Treated group	-31.4±9.7 (2.8±1.2)	<.0001

Values are the mean±SEM. *Wilcoxon rank sum test. Abbreviations are as in Table 2.

ized calcium, PTH, and 25-OHD levels remained unchanged in the 2 groups. Serum ionized calcium remained unchanged in the both groups. There was no significant difference between the 2 groups in the mean ± SD number of falls per subject during the 12 months (2.2±0.9 in the control group and 2.1±1.1 in the treatment group).

Adverse effects

Serious adverse events including death, overdose, and any other event that was life threatening or permanently disabling or that required intervention to prevent permanent impairment were not observed in either group. In the treatment group, 3 patients experienced gastrointestinal symptoms such as epigastric discomfort and nausea, 2 patients had esophagitis, and 2 patients experienced eruption of extremities, which eventually disappeared with appropriate therapy without discontinuation of the treatment. Three patients in the control group experienced headache, but this subsided within a week without discontinuing medication.

DISCUSSION

Prevention of fractures is one of the important issues in the management of elderly patients with AD. The high incidence of hip fractures in elderly patients with AD may be attributed to frequent falls [4] and osteoporosis due to low vitamin K1, and 25-OHD deficiency with compensatory hyperparathyroidism [11]. Indeed, serum levels of ucOC, 25-OHD and PTH and BMI were found to correlate with BMD in patients with AD.

Indeed, RRs for hip and nonvertebral fractures were low in the treatment group compared with the control group. This difference may be explained by a larger increase in BMD in the present study: the average values of BMD increased by 5.7% in the treatment group over 12 months. This may reflect a synergistic effect of menatetrenone and risedronate. The hip fracture rate in the control group was calculated as 87 per 1000 patient-years. The rate of hip fracture in an elderly reference population over ages 80 years was reported to be 22.9 per 1000 patient-years [33]. Although the mean age of our AD subjects (80.6 years) was within this range, the fracture rate in the present series was far higher than that reported in the reference population [33]. In addition to sunlight deprivation, 25-OHD deficiency and low vitamin K1 in these patients was considered to reflect generally poor nutrition, as also evidenced by lower BMIs. It has been reported that patients with dementia had malnutrition and decreased body weight [34]. Also, 25-OHD deficiency with compensatory hyperparathyroidism resulted in high urinary excretion of D-Pyr, which was corrected by risedronate in both groups. The decrease in bone turnover variables was more pronounced in the menatetrenone group, This may be caused by inhibition of bone resorption of menatetrenone [11].

In our previous study on stroke patients [35], with both vitamins D and K1 deficiency, treatment with menatetrenone for 1 year resulted in an increase in second metacarpal BMD by 4.3%, and the BMD in untreated controls decreased by 4.7%. Similar results were obtained by menatetrenone therapy in Parkinson's disease patients [36], and the odds ratio of nonvertebral fractures in the untreated controls and the menatetrenone group was 11.5 [36].

We conclude that AD patients with low serum vitamins K and D levels and high bone remodeling due to compensatory hyperparathyroidism are at an increased risk for nonvertebral fractures, particularly in the hip. Combined treatment with menatetrenone and risedronate may be safe and effective in increasing bone mass and reducing the risk of fractures in elderly patients with AD.

ACKNOWLEDGMENTS: This study was supported by a grant of Eizai Pharmaceuticals, Tokyo.

REFERENCES

1. Johansson C, and Skoog I. A population-based study on the association between dementia and hip fractures in 85-year olds. Aging (Milano) 1996; 8:189-196.
2. Melton LJ Ⅲ, Beard CM, Kokmen E, Atkinson EJ, and O'Fallon WM. Fracture risk in patients with Alzheimer's disease. J Am Geriatr Soc 1994; 42:614-619.
3. van Staa TP, Leufkens HG, and Cooper C. Utility of medical and drug history in fracture risk prediction among men and women. Bone 2002; 31:508-514.
4. Buchner DM, and Larson EB. Falls and fractures in patients with Alzheimer-type dementia. JAMA 1987; 257:1492-1495.
5. Nurmi I, Narinen A, Luthje P, and Tanninen S. Cost analysis of hip fracture treatment among the elderly for the public health services: a 1-year prospective study in 106 consecutive patients. Arch Orthop Trauma Surg 2003; 123:551-554.
6. Holmes J, and House A. Psychiatric illness predicts poor outcome after surgery for hip fracture: a prospective cohort study. Psychol Med 2000; 30:921-929.
7. Matsueda M, and Ishii Y. The relationship between dementia score and ambulatory level after hip fracture in the elderly. Am J Orthop 2000; 29:691-693.
8. Morrison RS, and Siu AL. Mortality from pneumonia and hip fractures in patients with advanced dementia. JAMA 2000; 284:2447-2448.
9. Nightingale S, Holmes J, Mason J, and House A. Psychiatric illness and mortality after hip fracture. Lancet 2001;

357:1264-1262.
10. Sato Y, Asoh T, and Oizumi K. High prevalence of vitamin D deficiency and reduced bone mass in elderly women with Alzheimer's disease. Bone 1998; 23:555-557.
11. Sato Y, Konoko T, Satoh K, and Iwamoto J. Menatetrenone and vitamin D2 with calcium supplements prevent nonvertebral fracture in elderly women with Alzheimer's disease. Bone 2005; 36:61-68.
12. Sato Y, Iwamoto J, Kanoko T, and Satoh K. The prevention of hip fracture with risedronate and ergocalciferol plus calcium supplementation in elderly women with Alzheimer disease. A randomized controlled trial. Arch Intern Med 2005; 165:1737-1742.
13. Presse N, Shatenstein B, Kergoat MJ, and Ferland G. Low vitamin K intakes in community-dwelling elders at an early stage of Alzheimer's disease. J Am Diet Assoc 2008; 108:2095-2099.
14. Sato Y, Honda Y, Hayashida N, Iwamoto J, Kanoko T et al. Vitamin K deficiency and osteopenia in elderly female patients with Alzheimer's disease. Arch Phys Med Rehabil 2005; 86:576-581.
15. Booth SL, Broe KE, Gagnon DR, Tucker KL, Hannan MT et al. Vitamin K intake and bone mineral density in women and men. Am J Clin Nutr 2003; 77:512-516.
16. Orimo H, Shiraki M, Tomita A, Morii H, Fujita T et al. Effects of menatetrenone on the bone and calcium metabolism in osteoporosis: A double-blind control-controlled study. J Bone Miner Metab 1998; 16:106-112.
17. Szulc P, Arlot M, Chapuy MC, Meunier PJ, and Delmas PD. Serum undercarboxylated osteocalcin correlates with hip bone mineral density in elderly women. J Bone Miner Res 1994; 9:1591-1595.
18. van Beek ER, Cohen LH, Leroy IM, Ebetino FH, Lowik CW et al. Differentiating the mechanisms of antiresorptive action of nitrogen containing bisphosphonates. Bone 2003; 33:805-811.
19. Reginster J, Minne HW, Sorensen OH, Hooper M, Roux C et al. Randomized trial of the effects of risedronate on vertebral fractures in women with established postmenopausal osteoporosis. Osteoporos Int 2000; 11:83-91.
20. Cranney 1 A, Waldegger L, Zytaruk N, Papaioannou A, Robinson VA et al. Risedronate for the prevention and treatment of postmenopausal osteoporosis. Cochrane Database Syst Rev 2003; 4:CD004523.
21. Sato Y, Kanoko T, Satoh K, and Iwamoto J. Risk factors for hip fracture among elderly patients with Alzheimer's disease. J Neurol Sci 2004; 223:107-112.
22. McKhann G, Drachman D, Folstein M, Katzman R, Price D et al. Clinical diagnosis of Alzheimer's disease: report on the NINCDS-ADRADA work group under the auspices of the Department of Health and Human Services. Task Force on Alzheimer's disease. Neurology 1984; 34:939-944.
23. Folstein MF, Folstein SF, and McHugh PR. "Mini Mental State." A practical method for grading the cognitive state of patients for the clinician. J Psychiatr Res 1975; 12:189-198.
24. Mahoney FI, and Barthel DW. Functional evaluation: the Barthel index. Md State Med J 1965; 14:61-65.
25. Rimm EB, Giovannucci EL, Stampfer MJ, Colditz GA, Litin LB et al. Reproducibility and validity of an expanded self-administered semiquantitative food frequency questionnaire among male health professionals. Am J Epidemiol 1992; 135:1114-1126.
26. Feskanich D, Weber P, Willett WC, Rockett H, Booth SL et al. Vitamin K intake and hip fractures in women: a prospective study. Am J Clin Nutr 1999; 69:74-79.
27. Komar L, Nieves J, Cosman F, Rubin A, Shen V et al. Calcium homeostasis of an elderly population upon admission to a nursing 1 home. J Am Geriatr Soc 1993; 41:1057-1064.
28. Matsumoto C, Kushida K, Yamazaki K, and Imose K, Inoue T. Metacarpal bone mass in normal and osteoporotic Japanese women using computed X-ray densitometry. Calcif Tissue Int 1994; 55:324-329.
29. Sato Y, Asoh T, Kaji M, and Oizumi K. Benefical effect of intermittent cyclical etidronate therapy in hemiplegic patients following an acute stroke. J Bone Miner Res 2000; 15:2487-2494.
30. Bügel S. Vitamin K and bone health in adult humans. Vitam Horm 2008; 78: 393- 416.
31. Hirao M, Hashimoto J, Ando W, Ono T, and Yoshikawa H. Response of serum carboxylated and undercarboxylated osteocalcin to alendronate monotherapy and combined therapy with vitamin K2 in postmenopausal women. J Bone Miner Metab 2008; 26:260-264.
32. Sagawa A. Undercarboxylated osteocalcin. Rheumatism 2007; 37;501-506.
33. Ramnemark A, and Nyberg L, Borssén B, Olsson T, and Gustafson Y. Fractures after stroke. Osteoporos Int 1998; 8:92-95.
34. Burns A, Marsh A, and Bender DA. Dietary intake and clinical, anthropometric and biochemical indices of malnutrition in elderly demented patients and non-demented subjects. Psychol Med 1989; 19:383-391.
35. Sato Y, Honda Y, Kuno H, and Oizumi K. Menatetrenone ameliorates osteopenia in disuse-affected limbs of vitamin D- and K- deficient stroke patients. Bone 1998; 23:291-296.
36. Sato Y, Honda Y, Kaji M, and Asoh T. Amelioration of osteoporosis by menatetrenone in elderly female Parkinson's disease patients with vitamin D deficiency. Bone 2002; 31:114-118.

Original Contribution

Kurume Medical Journal, 57, 125-132, 2010

Hybrid-Training Method Increases Muscle Strength and Mass in the Forearm without Adverse Effect of Hand Function in Healthy Male Subjects

HIROO MATSUSE, CHIKAHIRO IWASA, KISEI IMAISHI, TAKESHI NAGO, YOSHIHIKO TAGAWA*, TATSUYUKI KAKUMA** AND NAOTO SHIBA

*Rehabilitation Center, Kurume University Medical Center, Kurume 839-0863, *Department of Mechanical and Control Engineering, Kyushu Institute of Technology, Kitakyushu 804-8550 and **Biostatistics Center, Kurume University, Kurume 830-0011, Japan*

Received 28 July 2010, accepted 29 October 2010

Edited by NAOKO YOSHIDA

Summary: Conventional neuromuscular electrical stimulation (NMES) results in surface muscle contraction but high electrical stimulation intensity is required to activate the deep muscles. Therefore, NMES is not useful for training at complicated sites such as the forearm. To make NMES more effective we developed a hybrid training method (HYB), consisting of electrically stimulated antagonists to resist agonist muscle contractions. The purpose of this study was to compare the effects of HYB on the forearm as compared with NMES alone, and to determine whether HYB had any adverse effects on complex hand movements. Thirty subjects were randomly distributed into three groups: a HYB program group, an isometric electrical stimulation group (ES), and a control group (CN). Subjects trained 3 times a week for 6 weeks. Each session consisted of 10 sets of 10 reciprocal 2-sec wrist flexions and extensions separated by 1-min rest intervals. Wrist flexion\extension torques, grip strengths (GS), forearm flexor\extensor cross sectional areas (CSA), and hand dexterity (Purdue Pegboard (PEG) test, finger tapping (Tapping) test were measured. The HYB group demonstrated statistically significant increases in wrist extension torques (22.8%, $p<0.01$), forearm flexor CSA (9.6%, $p<0.01$), and in forearm extensor CSA (5.1%, $p<0.05$) at the end of training. There was no increase in torque or CSA in the ES or CN groups. Hand dexterity showed no significant differences in any of the three groups. HYB had no adverse effect on hand function and was more effective in forearm training than NMES alone.

Key words electrical stimulation, training, hand function, muscle strength

INTRODUCTION

Neuromuscular electrical stimulation (NMES) is widely used to lessen immobilization-associated muscle atrophy, to strengthen muscles, and to improve function in people with neuromuscular disabilities [1-5]. However, NMES has some limitations. For example, Henneman's size principle [6], (which states that in electrical stimulation activation occurs sequentially from Type I to Type Ⅱ fibers according to the training intensity seen in voluntary muscle contraction) is not seen in electrical stimulation [7]. NMES activation is nonselective with regard to the type of motor unit and synchrony, unlike voluntary contrac-

Corresponding author: Hiroo Matsuse MD PhD, Rehabilitation Center, Kurume University Medical Center, 155-1 Kokubu machi, Kurume 839-0863, Japan. Tel: 81-942-31-7568 Fax: 81-942-35-0709 E-mail: matsuse_hiroh@kurume-u.ac.jp

Abbreviations: Assembly, assembly test; BH, both hands; CN, control group; CSA, cross sectional areas; ES, electrical stimulation group; GS, grip strengths; HYB, hybrid training method; LH, left hand; MRI, magnetic resonance imaging; MVC, maximum voluntary cntraction; NMES, neuromuscular electrical stimulation; PEG, Purdue Pegboard; RLB, right plus left plus both hands; RH, right hand; ROM, range of motion; SD, standard deviation; Tapping, finger tapping; VC, voluntary muscular contractions.

tion [7,8]. Moreover NMES only stimulates the muscle on which the electrodes are placed, whereas voluntary movement implies activation from several synergic and stabilizer muscles, which are not stimulated by NMES [9]. These nonphysiologic patterns of activation may lead to less effective strengthening and may also contribute to the reluctance of many physicians to accept electric stimulation as a common component of therapeutic muscle strengthening programs. Also, it is generally reported that NMES evoked using surface electrodes results mainly in surface muscle contractions, and that it is hard to activate the deep muscles with this method [8,9]. Moreover NMES requires a high stimulation intensity to obtain an adequate muscle strengthening effect [8]. However high intensity NMES causes discomfort when used at sites with many superficial peripheral nerves or where cutaneous sensation is sensitive. Therefore stimulation intensity has been limited by subjects' tolerance [10]. The forearm is one of the sites where high stimulation intensity is problematic. A NMES method is needed that can provide an adequate muscular strengthening effect even at a comfortable, low stimulation intensities.

To make up for this limitation of NMES, a combined application of NMES and voluntary muscular contractions (VC) has been found effective and optimal in rehabilitation for immobilization or surgery [8,9]. Another new combined technique, the hybrid training method (HYB), has recently been developed (US patent 6,456,885.2002) [11]. This method resists the motion of VC agonist muscle with a force generated by an electrically stimulated antagonist. HYB was tested successfully for improving muscle strength and mass in healthy subjects [11-13]. Takano et al. [14] showed that HYB with low stimulation intensity increased strength and mass of the thigh muscles in elderly subjects.

An approach that can be used everywhere on the body is needed, because muscle weakness can occur anywhere. For example, in rheumatoid arthritis or aging, muscle weakness may occur in the upper extremities [15,16]. Especially in the hand and the forearm, not only muscle strength but also hand function decreases, so the effect of these training approaches on hand function must be considered [15]. High intensity exercise generally has a negative effect on hand function [16]. On the other hand, NMES does not facilitate intermuscular coordination [9]. Indeed, Vaz et al. [17] showed that NMES on wrist with hemiplegic cerebral palsy increased wrist strength without changing hand function. Moreover in a stroke patient's paretic (spastic) hand, NMES of Ia fibre in the extensor carpi radialis muscle is thought to induce reciprocal Ia-inhibition in the hand and finger flexors [18]. However, the effect of a combined application of NMES and VC on hand function and the specific coordination of complex movements is still unclear [8,9]. Therefore, it is necessary to examine whether HYB has an adverse effect on hand function when improving the muscle strength and hypertrophy in the forearm.

The present study was designed to compare the effect of HYB with NMES alone on the forearm in healthy subjects and to assess whether HYB for the forearm has an adverse influence on hand function.

MATERIALS AND METHODS

Participants

The Ethics Committee of Kurume University and the Japan Aerospace Exploration Agency approved the clinical design of this study protocol. Following approval, informed consent was obtained from a convenience sample of 30 healthy self-identified right hand dominant sedentary men (age, 21.4±2.5 (± standard deviation (SD)) yr; height, 171.6±4.8 cm; and weight, 63.4±8.4 kg) who had reviewed the goals of the study and agreed to participate. Inclusion criteria for the subjects were as follows; unremarkable musculoskeletal conditions, no adverse medical history, no excessive alcohol consumption and/or smoking, right hand (RH) dominant according to the Edinburgh Inventory [19], and having avoided participation in any strenuous or upper extremity specific sports activities for at least a year. Subjects meeting the above criteria were then randomized into three groups matched in age, in weight, and in height: the HYB Program Group (HYB, n=10) participated in a combined electrical stimulation-volitional contraction exercise program, the Electrical Stimulation Group (ES, n=10) took part in a conventional (isometric) NMES program, and the Control Group (CN, n=10) had no specific exercise program.

Intervention

Subjects attended a single familiarization session one month prior to beginning a 6-week 3-times-a-week (Monday, Wednesday, and Friday) training program. Each exercise session consisted of the participant being seated and voluntary or electrically performing 10 sets of 10 reciprocal wrist flexion and extension contractions with their non-dominant left upper extremity. Contractions were 2 sec in duration, and sets were separated by 1-min rest intervals. An

exercise session required 15 min and 40 sec to complete.

HYB Group: Exercises were performed in the seated position with the subject's radial and ulnar carpal flexor stimulated as the subject volitionally extended the wrist while opening the hand; next the reverse occurred (i.e., the radial and ulnar carpal extensor was stimulated) as the subject volitionally flexed the wrist while closing the hand. The range of motion of the joint was measured using a goniometer, and was restricted to an arc from a 45° wrist extension to a 45° wrist flexion. The subject changed the direction of the muscle contractions whenever they heard a tone emitted by the stimulator.

ES Group: These subjects were seated in the same posture as the HYB group described above. The procedures and number of sessions were identical to the HYB group with the exception that the subjects were instructed to avoid volitional contraction of the muscle; furthermore the left wrist was immobilized by a brace at the neutral position.

CN Group: Subjects did not exercise at all during this experiment period.

Equipment: The HYB apparatus consisted of an electrical stimulator, surface electrodes, and a joint motion sensor that triggered stimulation of the antagonist once it sensed the initiation of a volitional contraction [12]. Low impedance gel-coated electrodes (Sekisui plastics. Co., Ltd., Tokyo, Japan) placed over the motor points of the radial/ulnar carpal flexor and extensor have been previously described [11-14].

Waveform: Stimulation parameters were based on a standard Russian waveform in which a 5kHz carrier frequency was modulated at 20 Hz (2.4 ms on, 47.6 ms off) to deliver rectangular biphasic wave pulses [20].

Intensity: Stimulation intensities were set at the value of the threshold intensity plus two-thirds the difference between the maximum comfortable intensity and the threshold intensity [13], with the isometric contraction force limited to 25-30% of the maximum voluntary contraction (MVC). Output power was <10 W, the current intensity was <10 mA/cm^2, and the voltage was <80 V.

Evaluations

Measurements were performed at the baseline at the start of training as well as at the midpoint, and again at 6 weeks after the end of the exercise program, by a single blinded assessor.

Muscle Strength: Maximal isometric left wrist flexion and extension torques were obtained with the subject sitting in a CYBEX6000 (CSMI, MA, USA) apparatus with the left wrist positioned in the neutral position. Each subject was then asked to produce a maximal isometric wrist flexion and extension, and encouraged to monitor their own efforts on a video screen. The MVC was defined as the mean of three measurements at 5-min intervals.

Left grip strengths (GS) were measured with a hand-held Jamar dynamometer (Takei Kiki Kogyo Co., Ltd., Niigata, Japan) and defined as the mean of three measurements at 5-min intervals, using procedures recommended by the American Society of Hand Therapists [21-23].

Muscle mass: Cross sectional area (CSA)s in the forearm flexor and extensor were determined in conjunction with the torque evaluation sessions. The midpoint between the humeral lateral epicondyle and the radial styloid process was marke (Hitachi Medical Corp, Tokyo, Japan) with an indelible marker at the baseline evaluation and renewed as necessary throughout the experiment. A 5×5×5 mm magnetic resonance imaging (MRI) marker (Chugai Pharmaceutical Co., Ltd., Tokyo, Japan) was placed on the mark at the time of a CSA determination. Scout films were used to ensure that the scanning position did not change between sessions and images were collected as the subject lay with the upper extremity in a relaxed state. CSAs were measured by a blinded observer on the display of MRI scanner (Hitachi Medical Co., Tokyo, Japan).

Hand function: Two tests were used to assess different aspects of hand function. The standard version of the Purdue Pegboard (PEG) test was used to provide a global assessment of dexterity; Tiffin et al. [24,25] describe it in detail in their the manual. The PEG test provides separate sub-tests of the RH, left hand (LH), both hands (BH), right plus left plus both hands (RLB), and assembly test (Assembly) [28]. We took the three-trial administration procedures of the PEG test, and used average sub-test scores for our estimate [25,26]. The finger tapping (Tapping) test was used to assess speed of finger movements [26], and involved tapping the same key on a notebook computer with the index finger as fast as possible for ten sec of testing time, while not moving the wrist. The score was the number of times tapped.

Subjects were questioned about the occurrence of adverse effects at each session. Goniometric active and passive ranges of motion (ROM) as well as complaints of muscle pain were evaluated at the beginning and end of each session.

Data Analysis

A linear mixed model [27] was employed to com-

pare training effects on torques, GS, CSAs, PEG test scores and Tapping test scores between the three experimental groups. In the model, changes of measurements, (at the midpoint and endpoint of training) from the baseline were used as outcomes, physical characteristics (age, height and weight) and baseline scores were defined as co-variates, and random intercepts were included accounting for both heterogeneity of baseline measurements and serial correlation among repeated measurements. Comparison was made of the changes in measurements from the baseline within each group and between groups. Statistical analyses were performed with SAS software and p values ≤ 0.05 were considered to be statistically significant. Data are presented as means ± SD.

RESULTS

Muscle Strength

Wrist flexion torque (Fig. 1A): Maximal isometric wrist flexion torque in the HYB group increased from 12.8±4.1 Nm at the pre-training to 15.0±4.0 Nm at the end of training, however this increase was not significant. Maximal isometric wrist flexion torque did not change in the ES (from 13.8±5.0 Nm at pre-training to 14.1±3.0 Nm at the end of training) or CN groups (from 11.2±4.1 Nm at pre-training to 12.2±3.6 Nm at the end of training). No significant differences were observed between the groups.

Wrist extension torque (Fig. 1B): Maximal isometric wrist extension torque in the HYB group significantly increased from 11.4±3.7 Nm at pre-training to 14.0±3.1 Nm at the end of training ($p<0.01$). The maximal isometric wrist extension torque did not change in the ES (from 10.5±3.6 Nm at pre-training to 11.1±2.9 Nm at the end of training) or CN groups (from 11.6±3.2 Nm at pre-training to 10.3±3.1 Nm at the end of training). The increase of maximal isometric wrist extension torque was larger in the HYB group than in the CN group at the midpoint of the training ($p<0.01$) and at the endpoint of the training ($p<0.01$).

GS: There were no significant changes in GS for any of the three groups (Table 1).

Muscle mass

CSA of flexor (Fig. 2A): Forearm flexor CSA in the HYB group increased significantly from 13.4±2.5 cm^2 at pre-training to 14.4±3.0 cm^2 at the midpoint of training ($p<0.05$), and to 14.7±2.9 cm^2 at the end of training ($p<0.01$). Forearm flexor CSA did not change in the ES or CN groups, (13.4±2.5 cm^2 at pre-training

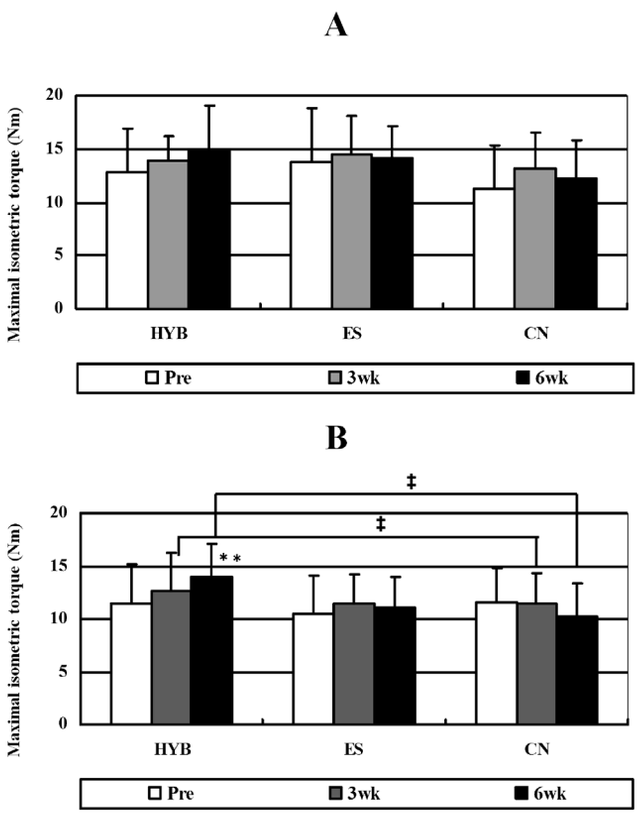

Fig. 1. Maximal isometric wrist flexion (A) and extension (B) torque production (Nm) at pre-training baseline as well as at the 3-week midpoint of training, and its 6-week conclusion. (A) Wrist flexion torque production had not increased in a statistically significant manner at the end of the 6-week training program in both the HYB and CN groups. Wrist extension torque production increased in the HYB groups by the end of training ($p<0.01$). (B) Both at the midpoint of training and at the end of training, there were statistically significant differences between the HYB and CN groups ($p<0.01$). Values are means ± SE. *Significant differences from pre-training value, $p<0.05$; **$p<0.01$. †Significant differences between the groups, $p<0.05$; ‡$p<0.01$. HYB, hybrid exercise method; ES, electrical stimulation; CN, control; Pre, pre-training; 3wk, 3-week; 6wk, 6-week.

TABLE 1.
Results of grip strengths (kg)

group	Pre mean (SD)	3wk mean (SD)	6wk mean (SD)
HYB	38.49 (4.37)	38.52 (3.35)	37.38 (3.86)
ES	41.07 (6.21)	40.89 (6.80)	40.72 (6.93)
CN	40.25 (4.90)	39.37 (4.82)	38.56 (7.40)

Values are means (SD), HYB, hybrid exercise method; ES, electrical stimulation; CN, control Pre, pre-training; 3wk, 3-week; 6wk, 6-week.

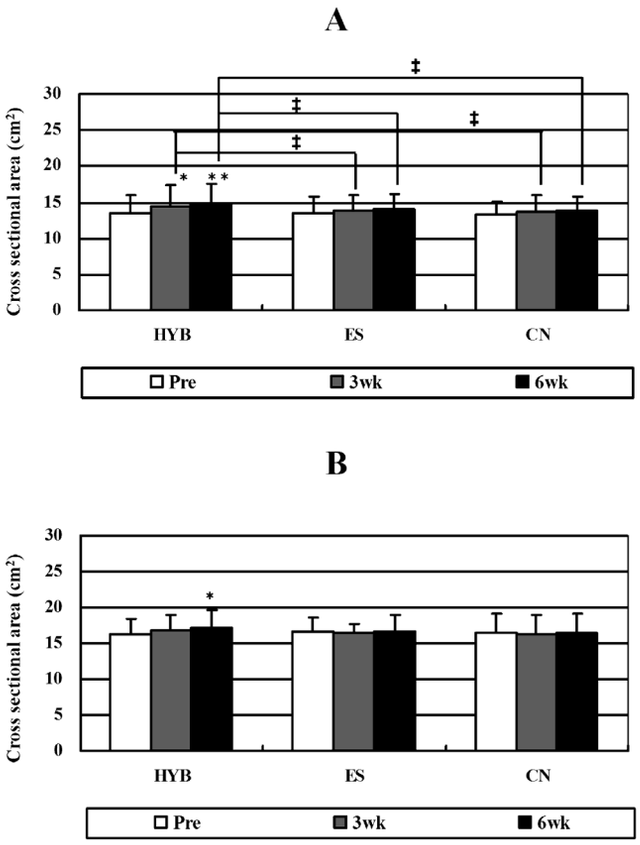

Fig. 2. Changes in the CSA (cm^2) of forearm flexor (A) and forearm extensor (B) at the pre-training baseline as well as at the 3-week midpoint, and the 6-week conclusion of training. The forearm flexor CSA increased in the HYB groups by the end of training ($p<0.01$). Both at the midpoint of training and at the end of training, there were statistically significant differences between the HYB and CN groups and between the HYB and ES groups, respectively ($p<0.01$). (A). Training effects on forearm extensor CSA were only evident in the HYB group statistically significant at the end of training ($p<0.05$) (B). Values are means ± SE. *Significant differences from pre-training value, $p<0.05$; **$p<0.01$. †Significant differences between the groups, $p<0.05$; ‡$p<0.01$. HYB, hybrid exercise method; ES, electrical stimulation; CN, control; Pre, pre-training; 3wk, 3-week; 6wk, 6-week.

to 14.1±2.2 cm^2 at the end of training, and 13.3±1.7 cm^2 at pre-training to 13.9±1.9 cm^2 at the end of training, respectively). The increase of the forearm flexor CSA in the HYB group was larger than that in the ES group or in the CN group at the midpoint of the training ($p<0.01$, for each group) and at the endpoint of the training ($p<0.01$, for each group).

CSA of extensor (Fig. 2B): The forearm extensor CSA in the HYB group increased significantly from 16.27±2.2 cm^2 at pre-training to 17.1±2.5 cm^2 at the end of training ($p<0.05$). The forearm extensor CSA did not increase from pre-training to the end of training in the ES or CN group (16.57±2.0 cm^2 to 16.62±2.3 cm^2 , and 16.4±2.6 cm^2 to 16.4±2.8 cm^2, respectively). There were no significant differences between the groups.

TABLE 2.
Results of Purdue Pegboard test and finger tapping test

group	test	Pre mean (SD)	3wk mean (SD)	6wk mean (SD)
HYB	RH	17.7 (1.16)	18.7 (1.34)	18.3 (1.64)
	LH	16.7 (1.77)	17.1 (1.85)	17.5 (1.51)
	BH	13.8 (1.18)	14 (1.40)	14.9 (1.14)
	RLB	47.8 (3.36)	48.5 (4.20)	50.5 (3.37)
	Assembly	45.1 (4.23)	48.6 (5.72)	49.3 (4.35)
	Tapping	62 (4.50)	60.9 (6.26)	60 (5.16)
ES	RH	16.8 (1.14)	17.8 (1.48)	17.8 (1.93)
	LH	15.8 (1.23)	16.3 (0.82)	16.8 (1.23)
	BH	13.5 (1.23)	13.8 (1.33)	14.2 (1.29)
	RLB	45.6 (2.72)	47.4 (4.81)	48.2 (3.65)
	Assembly	43.9 (3.84)	45 (5.45)	46.3 (7.03)
	Tapping	57.9 (4.99)	55.3 (5.27)	52.3 (2.80)
CN	RH	17.4 (1.58)	18 (2.00)	18.5 (1.72)
	LH	16.1 (1.10)	16.3 (1.83)	17 (1.05)
	BH	13.4 (0.84)	13.6 (1.71)	14.9 (1.60)
	RLB	46.5 (2.67)	47 (3.03)	49.7 (3.88)
	Assembly	45.4 (4.86)	43.8 (5.27)	45.9 (5.81)
	Tapping	58.5 (6.38)	57.4 (6.70)	56.4 (4.30)

Values are means (SD), HYB, hybrid exercise method; ES, electrical stimulation; CN, control; Assembly, assembly test; RH, right hand; LH. left hand; BH, both hands; RLB, right plus left plus both hand; Pre, pre-training; 3wk, 3-week; 6wk, 6-week.

Hand function

PEG and Tapping test: The scores of PEG test (RH, LH, BH, RLB, and Assembly) and Tapping test showed no significant changes within or among any of the three groups (Table 2).

The subjects tolerated training well and attended all training and evaluation sessions. There were no significant adverse events, and ROM was preserved in all groups. Four subjects in the HYB group complained of mild delayed onset muscle soreness during the first week of training, but recovered by the following week.

DISCUSSION

This study showed that HYB significantly increased wrist isometric extension torque and wrist muscle mass in both the flexor and extensor without having any

negative influence on hand functions. Although our sample size and the muscles studies were limited, these findings deserve further discussion.

It is well known that immobilization or disuse cause muscle atrophy, that is to say muscle mass, strength and endurance decrease [28-30]. Various training approaches are used in rehabilitation medicine to recover from immobilization or disuse. NMES is used widely to lessen immobilization-associated muscle weakness, to strengthen muscles, and to improve function in people with neuromuscular disabilities [1,19,28,32]. For example, the muscle strength of healthy subjects can be increased by 10% to 20% with 3 to 6 weeks of high-intensity stimulation [4,5]. Also, the usefulness of an electrically stimulated eccentric contraction was reported [33,34]. However, NMES has some limitations. NMES activates slow-twitch muscle poorly because Henneman's size principle is not seen in electrical stimulation [6]. Moreover, it is hard to activate the deep muscles using NMES with surface electrodes, and high electrical stimulation intensity causes discomfort. Therefore, combining NMES and VC can help overcome the limitations that occur when each is used in isolation, and is more effective for improving muscle properties [8,9]. HYB was developed as a new type of combined technique. It was reported effective in improving muscle strength and mass in healthy subjects [11-13]. This HYB obviates the weak point of NSEM because the use of both VC and ES makes it a more physiologic approach [11]. It is thought that the deep muscles that are difficult to stimulate by means of surface electrical stimulation are trained adequately by volitional contraction in HYB [11-14]. Also, HYB involves a combination of eccentric contractions and electric stimulation. Segar and Thorstensson [33] compared the effects of electrically stimulated eccentric, isometric, and concentric contractions of the quadriceps, and found that under similar stimulating conditions, eccentric contractions generated torques about 15% to 25% greater than those produced with isometric contractions and about 30% to 50% greater than the torques resulting from concentric contractions. Therefore, it has been considered that HYB increases muscle strength satisfactorily even at relatively low stimulation intensities. Indeed, Takano et al. [14] showed that HYB improved thigh muscle strength and hypertrophy in elderly people with a relatively low electrical stimulation intensity (equivalent to 20-25 repetition maximal). These advantages show that HYB is effective even for sites where high stimulation intensity is problematic, for example the forearm. The present study showed that HYB was effective in the forearm in healthy subjects, except with regard to GS and wrist flexion torque. On the other hand, NMES alone had no effect in the forearm at the same electrical stimulation intensity and frequency. Generally, the training effects of NMES are correlated to the stimulation intensity [8]. Because we made the electrical stimulation intensity weak enough to prevent discomfort, NMES would be ineffectiveness. The results of this study demonstrate that training became more effective when voluntary contractions were combined with NMES, even at a low electrical stimulation intensity (insufficient in NMES alone). In other words, HYB appears more efficient than NMES or VC alone.

NMES and VC induce different acute physiological effects on the neuromuscular system [9]. However, there it is not yet known how the combined application of NMES and VC influences neuromuscular systems. Therefore, HYB might induce an adverse influence on the neuromuscular system. Development of a training approach that can be used on all parts of the body is highly desirable because muscle weakness can occur anywhere in the body. Rehabilitation of the upper extremity is necessary not only for disuse but also for paralysis and rheumatoid arthritis. It has been reported that NMES is effective in paralysis [17,32] and rheumatoid arthritis [31]. In rehabilitation of the upper extremities (especially the forearm, hand, and finger), not only the effect of muscle strength but also the effect of hand function is very important [15,16]. Therefore the possible adverse influence on the specific coordination of complex movements needs to be considered in order to use HYB safely. Because NMES only stimulates the muscle on which the electrodes are placed, synergic and stabilizer muscles were not activated by NMES [9]. Paillard reported that NMES did not facilitate intermuscular coordination [9]. Indeed Vaz et al. [17] showed that NMES on wrist with hemiplegic cerebral palsy increased wrist strength without changing hand function. On the other hand, NMES of Ia fibre in the extensor carpi radialis muscle is thought to induce reciprocal Ia-inhibition in the hand and finger flexors in stroke patients [18]. Also, Maffiuletti et al. [35] reported that NMES in plantar flexor muscles did not affect alpha motoneuron excitability and/or presynaptic inhibition by examining maximal soleus and gastrocnemii H- and T-reflex. Voluntary training-induced modifications in H-reflex amplitude are usually ascribed to changes in alpha motoneuron excitability and/or changes in presynaptic inhibition of Ia afferents. However, these effects are not well understood in the combined technique. In the only report about the effect on H-reflex of HYB by Yamaguchi et al. [36],

they showed that the rate of change of the maximum soleus H-reflex to maximum soleus motor response in HYB was significantly higher than in conventional resistance training. They suggested that HYB was similar to co-contraction, and effects supraspinal and center mechanisms differently from conventional resistance training. If the specific coordination of complex movements in the upper extremity is disturbed by the combined technique, hand function would decline. In this study, we used PEG test and Tapping test to evaluate hand function, and results were not effected by HYB. This seems to show that HYB does not adversely affect the specific coordination of complex movements. Further research is necessary to reveal the effects on the neuromuscular system of the combined application of NMES and VC.

Isometric wrist flexion torque was not increased significantly in this study, because the wrist position might influence the measurement value [37]. Vaz et al. [17], in a study of NMES training on wrist muscles of children with hemiplegic cerebral palsy, reported that the isometric strength of flexors did not increase at the neutral position despite an increase of 30° in wrist extension, possibly reflecting shifts in the length-tension relationships due to functioning in altered muscle lengths. In the present study torque measurements were carried out in the neutral position, however there were no significant effects in either wrist isometric flexor strength or GS. Therefore the HYB program which was used in the current study might not be appropriate. The potential strength gain benefits are generally correlated to the intensity of the stimulation and the frequency of the training sessions [8]. It is possible that exercised in higher intensity the results might have varied. In HYB, the motion of a volitionally contracting agonist muscle against the force generated by its electrically stimulated antagonist shows an effect in the deep muscles where the electrical stimulation cannot reach. Influence on the deep muscles including the flexor digitorum profundus muscle which was important for GS might be ineffective in this study. Furthermore, because of the wrist flex action of their muscles, the increase of maximal isometric wrist flexion torque might lack statistical power even if the forearm flexor was significantly enlarged. Electrical stimulation intensity and the training frequency that we used in this study were set based on the maximum comfortable intensity we used in improving muscle strength and mass in the upper arm in a previous study [13]. However, this stimulation intensity appeared inadequate to increase muscle strength of grip and wrist flexor. Because the maximum comfortable intensity differs by stimulus site or subjects' tolerance, it may be desirable to set electrical stimulation intensity based on the repetition maximum as described by Takano et al. [14]. Voluntary wrist flexion exercise load can be increased by regulating electrical stimulation intensity of the carpal extensor. Improving the effectiveness of HYB is a problem for future study. In any case, HYB was effective in strengthening the wrist extensor without having negative influences on hand function (as a parameter of the neuromuscular system). It will be necessary to evaluate influences on different parts of the neuromuscular system with various HYB programs.

The current study was designed to assess the possible adverse effects of HYB on the specific coordination of complex movements, and it is the first study utilizing HYB for the forearm. To achieve more positive effects for the wrist, hand, and finger forces, it may be necessary to alter the present exercise program. Further research is necessary to refine HYB techniques and more clearly demonstrate the potential benefits for rehabilitation medicine.

CONCLUSIONS

HYB was capable of increasing muscle mass and strength without having any adverse influence on hand functions. This technique may be an effective and safe exercise technique for rehabilitation medicine.

ACKNOWLEDGMENTS: This study was supported in part by the Japanese Society for the Promotion of Science Grant-in-Aid for scientific research (14350138).

REFERENCES

1. Kagaya H, Shimada Y, and Ebata K. Restoration and analysis of standing-up in complete paraplegia utilizing functional electrical stimulation. Arch Phys Med Rehabil 1995; 76:876-881.
2. Delitto A, Rose SJ, McKowen JM, Lehman RC, Thomas JA et al. Electrical stimulation versus voluntary exercise in strengthening thigh musculature after anterior cruciate ligament surgery. Phys Ther 1988; 68:660-663.
3. Snyder-Mackler L, Delitto A, Bailey SL, and Stralka SW. Strength of the quadriceps femoris muscle and functional recovery after reconstruction of the anterior cruciate ligament. A prospective, randomized clinical trial of electrical stimulation. J Bone Joint Surg Am 1995; 77:1166-1173.
4. Balogum JA, Onilari OO, Akeju OA, and Marzouk DK. High voltage effects of pulse frequency. Arch Phys Med Rehabil 1993; 74:910-916.
5. Stein RB, Kimoto M, and Bobet J. Biomechanics of human quadriceps muscle during electrical stimulation. J Bionmech 1999; 32:347-353.
6. Henneman E, Somjen G, and Carpenter DO. Functional

significance of cell size in spinal motoneurons. J Neurophysiol 1965; 28:560-580.
7. Gregory CM, and Bickel CS. Recruitment patterns in human skeletal muscle during electrical stimulation. Phys Ther 2005; 85:358-364.
8. Dehail P, Duclos C, and Barat M. Electrical stimulation and muscle strengthening. Ann Readapt Med Phys 2008; 51:441-451.
9. Paillard T. Combined application of neuromuscular electrical stimulation and voluntary muscular contractions. Sports Med 2008; 38:161-177.
10. Cabric M, and Appell HJ. Effect of electrical stimulation of high and low frequency on maximum isometric force and some morphological characteristics in men. Int J Sports Med 1987; 8:256-260.
11. Yanagi T, Shiba N, Maeda T, Iwasa K, Umezu Y et al. Agonist contractions against electrically stimulated antagonists. Arch Phys Med Rehabil 2003; 84:843-848.
12. Iwasaki T, Shiba N, Matsuse H, Nago T, Umezu Y et al. Improvement in Knee Extension Strength through Training by Means of Combined Electrical Stimulation and Voluntary Muscle Contraction. Tohoku J Exp Med 2006; 209:33-40.
13. Matsuse H, Shiba N, Umezu Y, Nago T, Tagawa Y et al. Muscle training by means of combined electrical stimulation and volitional contraction. Aviat Space Environ Med 2006; 77:581-585.
14. Takano Y, Haneda Y, Maeda T, Sakai Y, Matsuse H et al. Increasing muscle strength and mass of thigh in elderly people with the hybrid-training method of electrical stimulation and volitional contraction. Tohoku J Exp Med 2010; 221:77-85.
15. Brorsson S, Hilliges M, Sollerman C, and Nilsdotter A. A six-week hand exercise programme improves strength and hand function in patients with rheumatoid arthritis. J Rehabil Med 2009; 41:338-342.
16. Olafsdottir HB, Zatsiorsky VM, and Latash ML. The effects of strength training on finger strength and hand dexterity in healthy elderly individuals. J Appl Physiol 2008; 105:1166-1178.
17. Vaz DV, Mancini MC, da Fonseca ST, Arantes NF, Pinto TB et al. Effects of strength training aided by electrical stimulation on wrist muscle characteristics and hand function of children with hemiplegic cerebral palsy. Phys Occup Ther Pediatr 2008; 28:309-325.
18. Hultborn H, Illert M, and Santini M. Convergence on interneurones mediating the reciprocal Ia inhibition of motoneurones. I. Disynaptic Ia inhibition of Ia inhibitory interneurones. Acta Physiol Scand. 1976; 96:193-201.
19. Oldfield RC. The assessment and analysis of handedness: the Edinburgh inventory. Neuropsychologia 1971; 9:97-113.
20. Ward AR, and Shkuratova N. Russian electrical stimulation: the early experiments. Phys Ther 2002; 82:1019-1030.
21. Fess EE. Clinical assessment recommendation. In: American Society of Hand Therapists Monograph (2nd ed.), Indianapolis, 1991.
22. Fess EE. The effect of Jamar dynamometer handle position and test protocol on normal grip strength. J Hand Surg 1982; 7A:308-309.
23. Hinson M, Woodard J, and Gench B. Reliability of the Jamar digital dynamometer model 2A. Occup Ther J Res 1990; 10:108-110.
24. Buddenberg LA, and Davis C. Test-retest reliability of the Purdue Pegboard Test. Am J Occup Ther. 2000; 54:558-558.
25. Tiffin J, and Asher EJ. The Purdue Pegboard; norms and studies of reliability and validity. J Appl Psychol 1948; 32:234-247.
26. Kee D, Morris K, Bathurst K, and Hellige JB. Lateralized interference in finger tapping: comparisons of rate and variability measures under speed and consistency tapping instructions. Brain Cogn 1986; 5:268-279.
27. Tokizane T. Studies on the paradoxical phase of sleep in the cat. In: Progress in Brain Research, ed. Tokizane T and Schade JP, Elsevier, Amsterdam, Vol 21B, pp 230-268, 1965.
28. Appell HJ. Muscular atrophy following immobilisation. A review. Sports Med 1990; 10:42-58.
29. Fiatarone MA, O'Neill EF, Ryan ND, Clements KM, Solares GR et al. Exercise training and nutritional supplementation for physical frailty in very elderly people. N Engl J Med 1994; 330:1769-1775.
30. Kozlovskaya IB, and Grigoriev AI. Russian system of countermeasures on board of the International Space Station (ISS): the first results. Acta Astronautica 2004; 55:233-237.
31. Brosseau LU, Pelland LU, Casimiro LY, Robinson VI, Tugwell PE et al. Electrical stimulation for the treatment of rheumatoid arthritis. Cochrane Database Syst Rev 2002; CD003687.
32. Hummelsheim H, Maier-Loth ML, and Eickhof C. The functional value of electrical muscle stimulation for the rehabilitation of the hand in stroke patients. Scand J Rehabil Med 1997; 29:3-10.
33. Segar JY, and Thorstensson A. Electrically evoked eccentric and concentric torque-velocity relationships in human knee extensor muscles. Acta Physiol Scand 2000; 169:63-69.
34. Westing SH, Segar JY, and Thorstensson A. Effects of electrical stimulation on eccentric and concentric torque-velocity relationships during knee extension in man. Acta Physiol Scand 1990;140:17-22.
35. Maffiuletti NA, Pensini M, Scaglioni G, Ferri A, Ballay Y et al. Effect of electromyostimulation training on soleus and gastrocnemii H- and T-reflex properties. Eur J Appl Physiol 2003; 90:601-607.
36. Yamaguchi T, Tanabe S, Watanabe T, and Muraoka Y. Effect of voluntary contraction with electrical stimulation to antagonist muscle on agonist H-reflex. Electromygr Clin Neurophysiol 2007; 47:251-255.
37. Bialocerkowski A, and Grimmer KA. Measurement of isometric wrist muscle strength--a systematic review of starting position and test protocol. Clin Rehabil 2003; 17:693-702.